Journal of Biotechnology 144 (2009) 287–292

Contents lists available at ScienceDirect

Journal of Biotechnology

journal homepage: www.elsevier.com/locate/jbiotec

Expression of human Cu, Zn-superoxide dismutase in an insect cell-free system and its structural analysis by MALDI-TOF MS

Toru Ezure[a,*], Takashi Suzuki[a], Eiji Ando[a], Osamu Nishimura[b], Susumu Tsunasawa[b]

[a] Clinical and Biotechnology Business Unit, Life Science Business Department, Analytical and Measuring Instruments Division, Shimadzu Corporation, 1 Nishinokyo-Kuwabaracho, Nakagyo-ku, Kyoto 604-8511, Japan
[b] Institute for Protein Research, Osaka University, 3-2 Yamadaoka, Suita-shi, Osaka 565-0871, Japan

ARTICLE INFO

Article history:
Received 27 July 2009
Received in revised form
14 September 2009
Accepted 21 September 2009

Keywords:
Cell-free protein synthesis system
Insect cell
Metalloprotein
hSOD1
MALDI-TOF MS

ABSTRACT

Human Cu, Zn-superoxide dismutase (hSOD1) is a homodimer that coordinates one copper and one zinc ion per monomer. These metal ions contribute to its enzymatic activity and structural stability. In addition, hSOD1 maintains an intra-subunit disulfide bond formed in the reducing environment of the cytosol and is active under a variety of stringent denaturing conditions. We report the expression of hSOD1 in a cell-free protein synthesis system constructed from *Spodoptera frugiperda* 21 (Sf21) insect cells, and its structural analysis including the status of the sole intra-subunit disulfide bond by mass spectrometry. By using this system hSOD1 was obtained in a soluble active form after addition of Cu^{2+} and Zn^{2+} and was purified with a yield of approximately 33 μg from 1 ml of reaction volume. Both enzymatic and structural analyses of the recombinant hSOD1 indicate that it was completely identical to the protein isolated from human erythrocytes.

1. Introduction

A large number of proteins require metal ions for their enzymatic activity and structural stability. Typical metals and their order of abundance in living organisms are iron, zinc, and copper, etc., and zinc ions are especially important for various proteins involved in diverse cellular processes. A recent bioinformatics report states that 2800 proteins corresponding to 10% of the human proteome are potentially zinc-binding (Andreini et al., 2006).

Cell-free protein synthesis systems allow us to optimize the reaction condition for each targeted protein by the addition of proper reagents. Therefore it is suitable for the synthesis of a protein that requires a co-factor for its enzymatic activity and/or structural stabilization. There are several reports regarding the expression of metalloproteins such as a heme protein from *Phanerochaete* (Miyazaki-Imamura et al., 2003) and a zinc-binding protein from *Arabidopsis* (Matsuda et al., 2006) using an *Escherichia coli* cell-free system, and it was reported that the proper concentration of metal ions in the reaction increased the solubility and yield of targeted metalloproteins. Though the heme protein was expressed in an active form after addition of hemin and various kinds of molecular chaperones, its structural analysis was not reported. Whereas the expression and characterization of plant-specific zinc-binding transcriptional factors have been well investigated, only the expression of the DNA binding domains, but not of the entire mature proteins, has been described.

A cell-free protein synthesis system (Transdirect *insect cell*) derived from Sf21 insect cells (Ezure et al., 2006; Suzuki et al., 2006a) has been developed as a tool for post-genomic studies to improve the efficiency of producing targeted proteins, especially in cases where it is difficult to obtain sufficient amounts for analyses, including measurement of enzymatic activity, western blotting and investigation of post-translational modifications such as N-terminal protein modifications (Suzuki et al., 2006b), protein prenylation (Suzuki et al., 2007) and formation of disulfide bonds (Ezure et al., 2007) by MS. Other post-translational modifications such as formation of protein complexes (Masuda et al., 2007) and ubiquitination (to be published elsewhere) also occurred in the insect cell-free system. In addition, core glycosylation and cleavages of signal peptides were observed after the addition of microsomal membranes to the reaction mixture (unpublished data). However, acquisition of metal ions has not been successful in this system. Therefore this insect cell-free system was used to examine the conditions required for optimal translation of hSOD1 as a model metalloprotein. hSOD1 exists in various organism and scavenges superoxide radicals to protect cells against oxidative stress. hSOD1 is a homodimeric enzyme that coordinates one copper and one zinc ion per monomer (McCord and Fridovich, 1969;

Abbreviations: CAT, chloramphenicol acetyltransferase; FALS, familial amyotrophic lateral sclerosis; hSOD1, human Cu, Zn-superoxide dismutase; PDI, protein disulfide isomerase; PMF, peptide mass fingerprinting; Sf21, *Spodoptera frugiperda* 21.

* Corresponding author. Tel.: +81 75 823 1351; fax: +81 75 823 1364.
E-mail address: ezure@shimadzu.co.jp (T. Ezure).

0168-1656/$ – see front matter © 2009 Elsevier B.V. All rights reserved.
doi:10.1016/j.jbiotec.2009.09.017

Forman and Fridovich, 1973; Briggs and Fee, 1978; Roe et al., 1988); the structural identity of recombinant hSOD1 was analyzed by MS and its structure and activity were compared with hSOD1 prepared from human erythrocytes. The present report demonstrates the expression of a metalloprotein in its mature form in a cell-free system and provides a detailed functional and structural analysis.

2. Materials and methods

2.1. Materials

Transdirect *insect cell* is a commercial product of Shimadzu (Kyoto, Japan). Restriction endonucleases and DNA modifying enzymes were purchased from TOYOBO (Osaka, Japan) and New England Biolabs, Inc. (Ipswich, MA). Desthiobiotin, TFA, CHCA and human SOD were from SIGMA (St. Louis, MO). *Strep*-Tactin superflow was from QIAGEN (Düsseldorf, Germany). Human cDNA clone hSOD1 (GenBank accession no. NM_000454) was obtained from TOYOBO. FluoroTect $Green_{Lys}$ tRNA was from Promega (Madison, WI).

2.2. Construction of plasmid

The expression plasmid for hSOD1 synthesis (pTD1-strep-hSOD1) was constructed as follows. The hSOD1 gene was amplified by PCR using the SOD-N primer (5′-ATGGCGACGAAGGCCG-3′) as the sense primer, the SOD-C primer (5′-GGGGTACCTTTTTGGGCGATCCCAATTACA-3′) as the antisense primer, and hSOD1 cDNA as the template. The amplified DNA fragment was then treated with T4 polynucleotide kinase. After digestion with *KpnI*, the amplified fragment was subcloned into the *EcoRV-KpnI* sites of a pTD1-strep vector (Ezure et al., 2007), and the resulting vector, pTD1-strep-hSOD1, containing hSOD1 having a *Strep*-tag at its C-terminus, was constructed.

For C6S/C111S double mutant synthesis, the expression plasmid (pTD1-strep-hSOD1-C6S/C111S) was constructed as follows. First, pTD1-strep-hSOD1-C6S was amplified by inverse PCR using the C6S-F primer (5′-GGCGACGGACCAGTGCAGG-3′) as the sense primer, the C6S-R primer (5′-CTTCAGCACGCTCACGGCCTT-3′) as the antisense primer, and pTD1-strep-hSOD1 as the template. After treatment with T4 polynucleotide kinase, the amplified fragment was allowed to self-ligate. Next, pTD1-strep-hSOD1-C6S/C111S was amplified by inverse PCR using the C111S-F primer (5′-TCAATCATTGGCCGCACACTGGT-3′) as the sense primer, the C111S-R primer (5′-ATGGTCTCCTGAGAGTGAGATCACA-3′) as the antisense primer, and pTD1-strep-hSOD1-C6S as the template. After treatment with T4 polynucleotide kinase, the amplified fragment was allowed to self-ligate.

pTD1-CAT (chloramphenicol acetyltransferase) was constructed using conventional cloning techniques. The DNA sequences of these recombinant constructs were confirmed by the dideoxynucleotide chain termination method.

2.3. Expression and fluorescent labeling of CAT

The mRNA was transcribed from pTD1-CAT and purified as described previously (Ezure et al., 2006). Cell-free protein synthesis was carried out using Transdirect *insect cell* in the presence over 0, 50, 100, 200, 400 and 800 μM $Cu(OAc)_2/Zn(OAc)_2$. Fluorescent labeling of *in vitro* translated proteins was carried out using FluoroTect $Green_{Lys}$ tRNA (Promega). 1 μl of FluoroTect was added to 50 μl of the reaction mixture. The reactions were carried out at 25 °C for 5 h. After the translation, an aliquot of the total fraction was centrifuged at 15,000 rpm for 15 min, and a supernatant fraction was obtained. 6 μl of these fractions were electrophoresed on 12.5% SDS-PAGE. The fluorescently labeled proteins were detected using a laser-based fluorescent scanner, Molecular Imager FX (Bio-Rad, Hercules, CA).

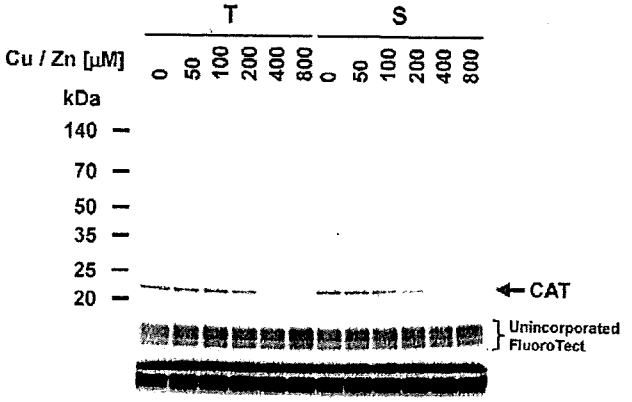

Fig. 1. SDS-PAGE analysis of CAT synthesized in the insect cell-free system. CAT was synthesized in the presence over 0, 50, 100, 200, 400 and 800 μM $Cu(OAc)_2/Zn(OAc)_2$. Fluorescent labeling of *in vitro* translated proteins was carried out as described in Section 2. 6 μl of the total (T) and supernatant (S) fractions were electrophoresed on 12.5% SDS-PAGE.

2.4. Expression and purification of hSOD1 and the hSOD1-C6S/C111S mutant

The mRNAs were synthesized and purified as described above. Cell-free protein synthesis was carried out at a 1 ml scale using Transdirect *insect cell* with or without the simultaneous addition of $Cu(OAc)_2$ and $Zn(OAc)_2$ to prepare equal final concentrations of Cu^{2+} and Zn^{2+} over the range of 1–400 μM. The reactions were carried out at 25 °C for 5 h, and the synthesized proteins were purified as described previously (Ezure et al., 2007). The proteins thus obtained were stored at −20 °C until use.

2.5. Measurement of enzymatic activity

SOD activity was determined using the SOD assay kit WST (Dojindo, Kumamoto, Japan) (Ukeda et al., 2002). One unit of SOD activity was defined as the amount of enzyme that inhibits the reaction of WST-1 (4-[3-(4-iodophenyl)-2-(4-nitrophenyl)-2H-5-

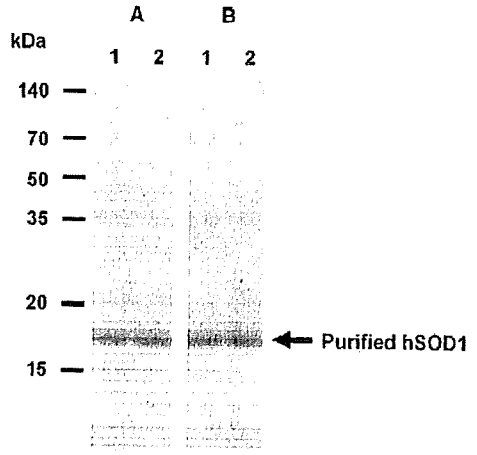

Fig. 2. SDS-PAGE analysis of purified wild-type and C6S/C111S mutant hSOD1s synthesized in the insect cell-free system under optimal conditions. The synthesized proteins were purified using a *Strep*-Tactin superflow column as described previously (Ezure et al., 2007). The purified proteins (1 μg) were electrophoresed on 15% SDS-PAGE under (A) reducing and (B) non-reducing conditions. Lanes 1 and 2: wild-type and C6S/C111S mutant hSOD1s, respectively.

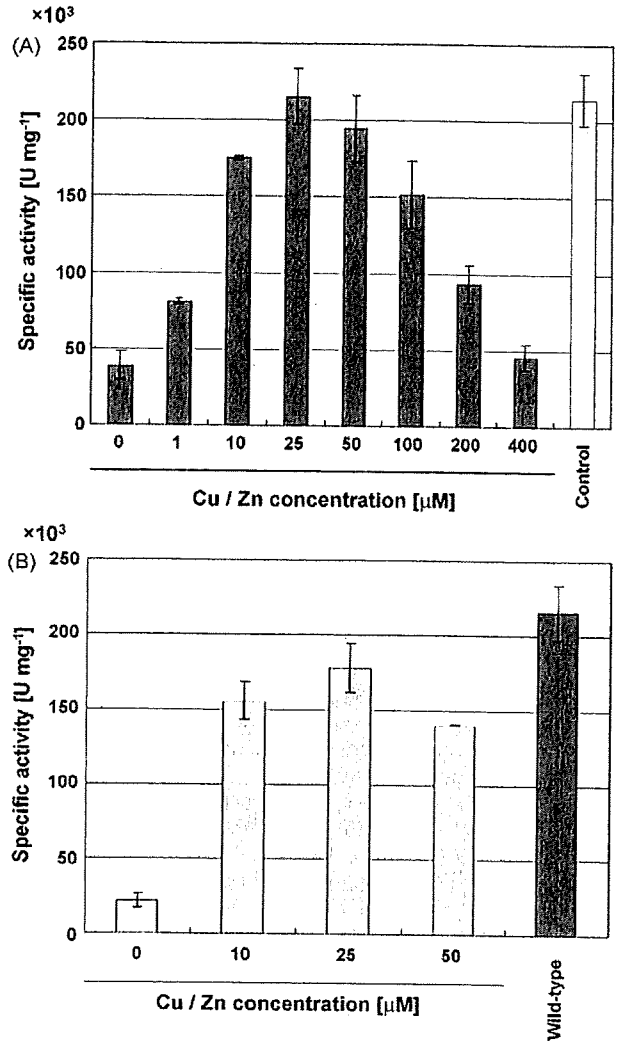

Fig. 3. Specific activities of wild-type (A) and C6S/C111S mutant (B) hSOD1s synthesized in the insect cell-free system after simultaneous addition of various concentrations of Cu/Zn ions. Control was the authentic hSOD1 purified from human erythrocytes, and wild-type indicates the hSOD1 synthesized in the cell-free system under optimal conditions. The means and standard deviations of three replicate experiments are indicated.

tetrazolio]-1,3-benzene disulfonate sodium salt) with superoxide anion by 50% at 37 °C for 20 min.

2.6. Protein assay

The protein concentration was quantified using the QuantiPro™ BCA Assay Kit (SIGMA). Bovine serum albumin was used as the standard protein.

2.7. Confirmation of amino acid sequence and disulfide status of hSOD1 by MALDI-TOF MS

The purified wild-type and C6S/C111S mutant hSOD1s (each 10 μg) were denatured in 10 μl of 8 M urea solution and then submitted to one of the three following conditions: (a) reduction with DTT followed by *S*-alkylation with iodoacetamide, (b) *S*-alkylation with iodoacetamide and (c) no treatment. Each reaction mixture was diluted by adding 90 μl of 50 mM ammonium bicarbonate and was then digested with trypsin (350 ng, Promega) overnight. The resulting tryptic digests were desalted and concentrated to approximately 8 μl by ZipTip μ-C18 (Millipore, Billerica, MA). Aliquots of samples (each 0.5 μl) were each mixed with 0.5 μl of CHCA solution (5 mg ml^{-1} in 50% (v/v) acetonitrile containing 0.1% (v/v) TFA) on the MALDI target plate and analyzed. The mass spectra of the tryptic digests were acquired in reflectron positive ion mode with an AXIMA-CFR™-plus MALDI-TOF MS instrument (Shimadzu/Kratos, Manchester, UK) according to a standard method (Yamaguchi et al., 2005).

3. Results and discussion

3.1. Effect of metal ions on the insect cell-free protein synthesis

Matsuda et al. (2006) synthesized CAT in the presence of zinc ion to confirm the effect of zinc ion on an *E. coli* cell-free system. For the same purpose, CAT was synthesized in the insect cell-free system by simultaneously adding equal amounts of $Cu(OAc)_2$ and $Zn(OAc)_2$ utilizing a fluorescence labeling method, and the yield and solubility of the resulting proteins were analyzed by SDS-PAGE. As the concentrations of both metal ions were increased, CAT synthesis was gradually inhibited and its yield decreased (Fig. 1). A similar phenomenon was observed using an *E. coli* cell-free system (Matsuda et al., 2006). Taking into consideration the fact that the concentrations of metal ions such as Cu^{2+} and Zn^{2+} have little effect in general on protein solubility, this suggests that these ions might have essentially inhibitory effects on the cell-free protein synthesis.

3.2. Expression, purification and characterization of hSOD1

Wild-type hSOD1 proteins synthesized at various concentrations of metal ions were purified by affinity column chromatography, and their purities were judged by SDS-PAGE with or without reducing reagent followed by staining with CBB (Fig. 2, lane 1). Each purified protein ran as nearly a single band having a molecular mass of about 18 kDa, regardless of the presence or absence of a reducing reagent. Each apparent molecular mass was compatible with the theoretical value calculated from the amino acid sequence of hSOD1. These results suggest that hSOD1 proteins expressed in this cell-free system do not form an inter-subunit disulfide bond as in the authentic hSOD1, despite the existence of two sulfhydryl groups per subunit.

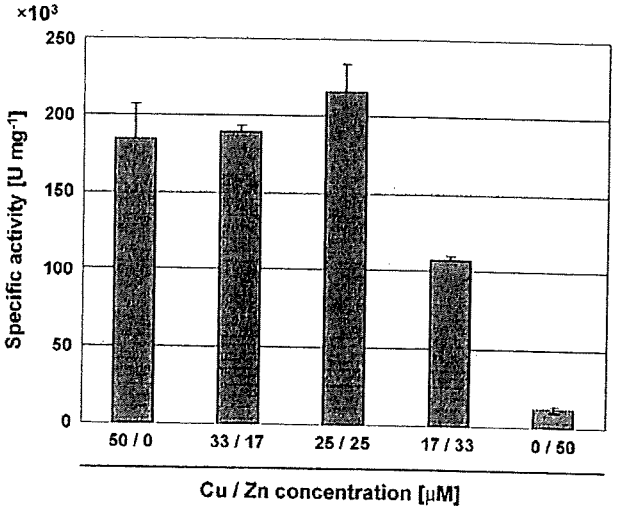

Fig. 4. Specific activities of wild-type hSOD1 synthesized in the insect cell-free system after simultaneous addition of various ratios of Cu/Zn ions. Total concentration of Cu^{2+} and Zn^{2+} was set at 50 μM. The means and standard deviations of three replicate experiments are indicated.

(M)[1]ATKAVCVLKG DGPVQGIINF EQKESNGPVK VWGSIKGLTE GLHGFHVHEF[50]
[51]GDNTAGCTSA GPHFNPLSRK HGGPKDEERH VGDLGNVTAD KDGVADVSIE[100]
[101]DSVISLSGDH CIIGRTLVVH EKADDLGKGG NEESTKTGNA GSRLACGVIG[150]
[151]IAQKGTGSGG GGGGGGWSHP QFEK
Spacer sequence Strep-tag sequence

Fig. 5. Amino acid sequence of the authentic hSOD1 and the location of its disulfide bond. Disulfide linkage of hSOD1 is indicated by a line. Spacer and *Strep*-tag sequences are underlined. The regions which were not detected in the PMF analysis of wild-type hSOD1 are indicated by a dotted line.

Similar to the expression of CAT, the yields of hSOD1 proteins depended on the concentrations of metal ions. The simultaneous addition of $Cu(OAc)_2$ and $Zn(OAc)_2$ at final concentrations of 200–400 μM significantly decreased the yields of hSOD1s (data not shown), whereas by simultaneous addition of $Cu(OAc)_2$ and $Zn(OAc)_2$ at final concentrations of 25 μM, hSOD1 produced the highest specific activity (Fig. 3A). This value (215,788.7 ± 17,965.8 units mg^{-1}) was almost equal to that of the authentic hSOD1 protein (214,188.7 ± 16,915.0 units mg^{-1}), which was produced with a final yield of 33 μg from 1 ml of the reaction mixture. It has been reported that for hSOD1 synthesis using *in vivo* expression systems such as *E. coli* (Hartman et al., 1986), yeast (Hallewell et al., 1987) and baculovirus (Fujii et al., 1995), the concentration of Cu^{2+} affects only the yield of the active form of the protein, because the medium contains sufficient Zn^{2+}. To confirm the optimum ratio of added Cu^{2+} and Zn^{2+} in the insect cell-free system, hSOD1 proteins were synthesized at various ratios of metal ions. Total concentration of Cu^{2+} and Zn^{2+} was set at 50 μM. The optimal ratio of added Cu^{2+} and Zn^{2+} was 1:1 (Fig. 4), suggesting that the optimal ratio of Cu^{2+} and Zn^{2+} corresponds to that incorporated into the targeted protein, because metal ion concentration were controlled in the cell-free system. Whereas 85.5% of the specific activity at the optimum ratio was observed by only addition of $Cu(OAc)_2$ at final concentration of 50 μM, hSOD1 produced low activity by only addition of $Zn(OAc)_2$. These results indicated that cupper plays the main role of hSOD1 activity as reported (Rae et al., 2001). Furthermore, there are several reports regarding the reconstitution of hSOD1 in its apo-form (Jewett et al., 1982; Yamazaki and Takao, 2008). Though this method might be suitable for stable proteins such as hSOD1, it should be emphasized that the co-translational method described here is very useful for synthesis of various eukaryotic metalloproteins in the proteomic era.

3.3. Confirmation of the amino acid sequence of hSOD1 synthesized in the insect cell-free system and location(s) of disulfide bond(s)

To confirm the amino acid sequence and location(s) of the disulfide bond(s) of wild-type hSOD1 synthesized in the insect cell-free system, the protein was analyzed by MALDI-TOF MS. Fig. 5 shows the location of a disulfide bond for the authentic protein along with its complete amino acid sequence. The purified recombinant protein was treated under one of the three following conditions: (a) reduction followed by *S*-alkylation with iodoacetamide, (b) *S*-alkylation with iodoacetamide, and (c) no treatment, followed by tryptic digestion. Resulting tryptic peptides from each treatment were analyzed by MALDI-TOF MS. The peptide mass fingerprinting (PMF) for each protein sample was identical, with the exception of regions corresponding to cysteine-containing peptides, regardless of sample treatment conditions, and the values obtained were in good agreement with the theoretical values calculated from the authentic protein assuming the presence of a disulfide bond between residues 57 and 146, plus two carbamidomethyl-cysteines at positions 6 and 111 resulting from *S*-alkylation treatment using iodoacetamide (Table 1). Thus, 75.9% of the sequence coverage on PMF was observed for each purified protein sample, i.e. the amino acid sequence of 132 of the total 174 residues (Fig. 5). This result strongly indicates that the protein is identical to the authentic hSOD1.

For protein samples treated with *S*-alkylation, regardless of reduction, three peaks that apparently corresponded to tryptic fragments containing carbamidomethyl-cysteine were observed at *m/z* values 2171.87, 2514.33 and 3720.94. These values were in good agreement with the theoretical values (*m/z* 2172.15, 2514.21, 3720.81) calculated from the amino acid sequence of the authentic protein. Furthermore, for the protein that was not treated

Table 1
Theoretical and observed monoisotopic mass values for tryptic digests of hSOD1.

Mass value	Position	Modification(s)	Modified mass value	Observed mass value[a]			Peptide sequence
				(a)	(b)	(c)	
632.38	4–9	Cys_CAM[c]: 6	689.40	689.43		632.38	AVCVLK
1501.76	10–23				1501.89		GDGPVQGIINFEQK
2115.13	4–23 (MC[b]:1)	Cys_CAM: 6	2172.15	2171.87		2115.44	AVCVLKGDGPVQGIINFEQK
730.37	24–30				N.D.[d]		ESNGPVK
689.40	31–36				689.43		VWGSIK
3462.60	37–69	Cys_CAM: 57	3519.62	3519.74		N.D.	GLTEGIHGFHVHEFGDNTAGCTSAGPHFNPLSR
1225.62	80–91				1225.71		HVGDLGNVTADK
2457.19	92–115	Cys_CAM: 111	2514.21	2514.33		2457.49	DGVADVSIEDSVISLSGDHCIIGR
3663.79	80–115 (MC:1)	Cys_CAM: 111	3720.81	3720.94		3663.93	HVGDLGNVTADKDGVADVSIEDSVISLSGDHCIIGR
825.48	116–122				825.53		TLVVHEK
618.31	123–128				N.D.		ADDLGK
821.36	129–136				N.D.		GGNEESTK
662.32	137–143				N.D.		TGNAGSR
1072.62	144–154	Cys_CAM: 146	1129.64	1129.73		N.D.	LACGVIGIAQK
1816.80	155–174				1816.97		GTGSGGGGGGGGWSHPQFEK

Mass values over 600 are shown.
[a] (a)-(c) stand for the sample conditions described in Section 2.
[b] MC stands for the number of missed cleavages.
[c] Cys_CAM stands for carbamidomethyl-cysteine.
[d] Not detected.

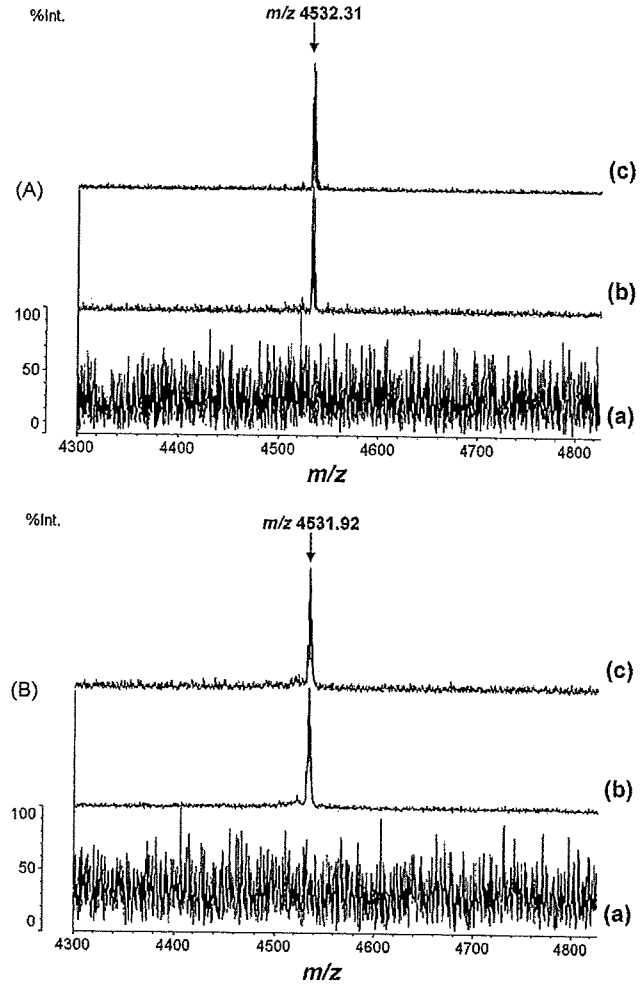

Fig. 6. MALDI-mass spectra of tryptic digests of wild-type (A) and C6S/C111S mutant (B) hSOD1s. The acquired profiles were focused on mass ranges from 4300 to 4800. The purified hSOD1s were treated under the following three conditions: (a) reduction and *S*-alkylation, (b) *S*-alkylation, and (c) no treatment. Arrow and numerical value indicate specific peptide peak and observed mass, respectively.

with *S*-alkylation, peaks having *m/z* values of 2115.44, 2457.49 and 3663.93, instead of the three peaks described above, were observed. Each value was in good agreement with the theoretical value (*m/z* 2115.13, 2457.19, 3663.79) calculated from the tryptic peptide fragments containing un-modified cysteines (corresponding to residue No.6 and No.111). The results clearly showed that Cys^6 and Cys^{111} in the protein synthesized in this system did not form a disulfide bond.

On the other hand, in the case of the reduced and *S*-alkylated protein, two peaks were clearly observed at *m/z* values of 3519.74 and 1129.73, which were in good agreement with the theoretical values (3519.62 and 1129.64) assuming that each peptide contained a carbamidomethyl-cysteine at residue No. 57 and No. 146, respectively. However, these peaks were not detected for the non-reduced *S*-alkylated hSOD1 or for the untreated protein, and a peak at *m/z* value of 4532.31 was observed (Fig. 6A), which was in good agreement with the theoretical value (4532.22) calculated from a tryptic peptide predicted for a protein with a disulfide linkage between Cys^{57} and Cys^{146} (Table 2).

No peaks corresponding to predicted values for any other disulfide linkages were detected, indicating that the wild-type hSOD1 synthesized in the insect cell-free system has a highly conserved pair of cysteines (Cys^{57} and Cys^{146}) that form an intra-subunit disulfide bond as well as two free cysteines (Cys^6 and Cys^{111}) similar to the hSOD1 from human erythrocytes (Lepock et al., 1990; Parge et al., 1992; Arnesano et al., 2004; Lindberg et al., 2004).

3.4. Enzymatic and structural analyses of the hSOD1 C6S/C111S mutant synthesized using the insect cell-free system

To confirm the contribution of two free cysteines (Cys^6 and Cys^{111}) to the enzymatic activity of hSOD1 and the disulfide bond formation, a C6S/C111S double mutant, in which two free cysteines were replaced by serine, was constructed. The C6S/C111S mutant was synthesized and purified (Fig. 2, lane 2). As in the synthesis of wild-type hSOD1, the simultaneous addition of $Cu(OAc)_2$ and $Zn(OAc)_2$ at final concentrations of 25 μM Cu^{2+} and Zn^{2+} was optimal for the enzymatic activity of the C6S/C111S mutant (Fig. 3B), although its specific activity (178,335.3 ± 16,087.8 units mg^{-1}) was slightly less than that of the wild-type protein (215,788.7 ± 17,965.8 units mg^{-1}). However, MALDI-TOF MS analysis demonstrated that this mutant, when synthesized under the optimized conditions, formed a disulfide linkage between Cys^{57} and Cys^{146} similar to the wild-type hSOD1 (Fig. 6B). The results indicated that two free cysteine residues, Cys^6 and Cys^{111}, had little effect on the SOD activity as reported (Parge et al., 1992; Arnesano et al., 2004), and that they were not involved in disulfide formation.

Recently, hSOD1 have attracted attention because familial amyotrophic lateral sclerosis (FALS) is possibly caused by the aggregation of hSOD1. It is suggested that some mutations in region of interface cause dissociation of a dimer to a monomer (Deng et al., 1993). A lot of mutations have been identified in patients with FALS. Therefore, the method of mutagenesis analysis described above could be useful tool for the preparation of hSOD1 mutants.

In order to become enzymatically active by forming the correctly folded quaternary structure, several post-translational modifications of hSOD1 are required, including acquisition of a 1:1 molar ratio of copper and zinc ions, respectively, formation of an intra-subunit disulfide bond, and dimerization. The insertion of copper by a copper chaperone for SOD1 is well established (Rae et al., 2001; Torres et al., 2001; Bartnikas and Gitlin, 2003; Furukawa et al., 2004), but the mechanism by which SOD1 acquires a zinc ion is not fully understood. The formation of a disulfide bond is a peculiar event for a cytosolic protein, because the cytosol is a strongly reducing environment. However, proteins containing disulfide bonds were expressed successfully using the insect cell-free system under

Table 2
Theoretical and observed monoisotopic mass values for disulfide-linked peptides.

Mass value	Position	MC[a]	Modification(s)	Modified mass value	Observed mass value	Peptide sequence[b]
3462.60	37–69	0	Disulfide bond: 57–146	4532.22	4532.31	GLTEGLHGFHVHEFGDNTAGCTSAGPHFNPLSR
1072.62	144–154	0				LACGVIGIAQK

[a] MC stands for the number of missed cleavages.
[b] Disulfide linkage is indicated by a line.

non-reducing conditions after addition of reduced glutathione, oxidized glutathione, and protein disulfide isomerase (PDI) in a previous study (Ezure et al., 2007). In the cell-free system using non-reducing conditions as described above, hSOD1 was synthesized but was insoluble, and its specific activity remained less than 15% that of the authentic hSOD1, even after addition of metal ions, and only a band corresponding to the monomer form was observed on SDS-PAGE analysis without a reducing reagent (data not shown). From these data, we concluded that a random inter-subunit disulfide bond could not be formed under these conditions. Normally, the formation and isomerization of disulfide bonds is catalyzed by PDI in the lumen of the endoplasmic reticula. In a previous study, this situation was reconstituted in the insect cell-free system. Because the secreted protein human lysozyme was used as a model protein in a previous study, it is supposed that this could be a suitable expression system. However, optimal expression conditions may differ according to the localization and disulfide status of targeted proteins.

In conclusion, the present study, by demonstrating that an active metalloprotein could be synthesized under optimized conditions using an insect cell-free protein synthesis system, shows that this system can effectively synthesize proteins that require metal ions for their correct quaternary structures and for their enzymatic activities.

Acknowledgements

We thank Dr. Minoru Yamaguchi and Mr. Shin-ichiro Kobayashi, Shimadzu Corporation, for helpful discussions of peptide preparations and mass spectrometric analyses. We are grateful to Dr. Yuzo Yamazaki, Shimadzu Corporation, for helpful discussions of SOD1.

References

Andreini, C., Banci, L., Bertini, I., Rosato, A., 2006. Counting the zinc-proteins encoded in the human genome. J. Proteome Res. 5, 196–201.

Arnesano, F., Banci, L., Bertini, I., Martinelli, M., Furukawa, Y., O'Halloran, T.V., 2004. The unusually stable quaternary structure of human Cu, Zn-superoxide dismutase 1 is controlled by both metal occupancy and disulfide status. J. Biol. Chem. 279, 47998–48003.

Bartnikas, T.B., Gitlin, J.D., 2003. Mechanisms of biosynthesis of mammalian copper/zinc superoxide dismutase. J. Biol. Chem. 278, 33602–33608.

Briggs, R.G., Fee, J.A., 1978. Further characterization of human erythrocyte superoxide dismutase. Biochim. Biophys. Acta 537, 86–99.

Deng, H.X., Hentati, A., Tainer, J.A., Iqbal, Z., Cayabyab, A., Hung, W.Y., Getzoff, E.D., Hu, P., Herzfeldt, B., Roos, R.P., Warner, C., Deng, G., Soriano, E., Smyth, C., Parge, H.E., Ahmed, A., Roses, A.D., Hallewell, R.A., Pericak-Vance, M.A., Siddique, T., 1993. Amyotrophic lateral sclerosis and structural defects in Cu, Zn superoxide dismutase. Science 261, 1047–1051.

Ezure, T., Suzuki, T., Higashide, S., Shintani, E., Endo, K., Kobayashi, S., Shikata, M., Ito, M., Tanimizu, K., Nishimura, O., 2006. Cell-free protein synthesis system prepared from insect cells by freeze-thawing. Biotechnol. Prog. 22, 1570–1577.

Ezure, T., Suzuki, T., Shikata, M., Ito, M., Ando, E., Nishimura, O., Tsunasawa, S., 2007. Expression of proteins containing disulfide bonds in an insect cell-free system and confirmation of their arrangements by MALDI-TOF mass spectrometry. Proteomics 7, 4424–4434.

Forman, H.J., Fridovich, I., 1973. On the stability of bovine superoxide dismutase. The effects of metals. J. Biol. Chem. 248, 2645–2649.

Fujii, J., Myint, T., Seo, H.G., Kayanoki, Y., Ikeda, Y., Taniguchi, N., 1995. Characterization of wild-type and amyotrophic lateral sclerosis-related mutant Cu, Zn-superoxide dismutases overproduced in baculovirus-infected insect cells. J. Neurochem. 64, 1456–1461.

Furukawa, Y., Torres, A.S., O'Halloran, T.V., 2004. Oxygen-induced maturation of SOD1: a key role for disulfide formation by the copper chaperone CCS. EMBO J. 23, 2872–2881.

Hallewell, R.A., Mills, R., Tekarmp-Olson, P., Blacher, R., Rosenbarg, S., Ottng, F., Masiarz, F., Scandella, D.J., 1987. Amino terminal acetylation of authentic human Cu, Zn-superoxide dismutase produced in yeast. Biotechnology 5, 363–366.

Hartman, J.R., Geller, T., Yavin, Z., Bartfeld, D., Kanner, D., Aviv, H., Gorecki, M., 1986. High-level expression of enzymatically active human Cu/Zn superoxide dismutase in *Escherichia coli*. Proc. Natl. Acad. Sci. U.S.A. 83, 7142–7146.

Jewett, S.L., Latrenta, G.S., Beck, C.M., 1982. Metal-deficient copper-zinc superoxide dismutases. Arch. Biochem. Biophys. 215, 116–128.

Lepock, J.R., Frey, H.E., Hallewell, R.A., 1990. Contribution of conformational stability and reversibility of unfolding to the increased thermostability of human and bovine superoxide dismutase mutated at free cysteines. J. Biol. Chem. 265, 21612–21618.

Lindberg, M.J., Normark, J., Holmgren, A., Oliveberg, M., 2004. Folding of human superoxide dismutase: disulfide reduction prevents dimerization and produces marginally stable monomers. Proc. Natl. Acad. Sci. U.S.A. 101, 15893–15898.

Masuda, T., Goto, F., Yoshihara, T., Ezure, T., Suzuki, T., Kobayashi, S., Shikata, M., Utsumi, S., 2007. Construction of homo- and heteropolymers of plant ferritin subunits using an in vitro protein expression system. Protein Expr. Purif. 56, 237–246.

Matsuda, T., Kigawa, T., Koshiba, S., Inoue, M., Aoki, M., Yamasaki, K., Seki, M., Shinozaki, K., Yokoyama, S., 2006. Cell-free synthesis of zinc-binding proteins. J. Struct. Funct. Genomics 7, 93–100.

McCord, J.M., Fridovich, I., 1969. Superoxide dismutase. An enzymic function for erythrocuprein (hemocuprein). J. Biol. Chem. 244, 6049–6055.

Miyazaki-Imamura, C., Oohira, K., Kitagawa, R., Nakano, H., Yamane, T., Takahashi, H., 2003. Improvement of H_2O_2 stability of manganese peroxidase by combinatorial mutagenesis and high-throughput screening using *in vitro* expression with protein disulfide isomerase. Protein Eng. 16, 423–428.

Parge, H.E., Hallewell, R.A., Tainer, J.A., 1992. Atomic structures of wild-type and thermostable mutant recombinant human Cu, Zn superoxide dismutase. Proc. Natl. Acad. Sci. U.S.A. 89, 6109–6113.

Rae, T.D., Torres, A.S., Pufahl, R.A., O'Halloran, T.V., 2001. Mechanism of Cu, Zn-superoxide dismutase activation by the human metallochaperone hCCS. J. Biol. Chem. 276, 5166–5176.

Roe, J.A., Butler, A., Scholler, D.M., Valentine, J.S., Marky, L., Breslauer, K.J., 1988. Differential scanning calorimetry of Cu, Zn-superoxide dismutase, the apoprotein, and its zinc-substituted derivatives. Biochemistry 27, 950–958.

Suzuki, T., Ito, M., Ezure, T., Kobayashi, S., Shikata, M., Tanimizu, K., Nishimura, O., 2006a. Performance of expression vector, pTD1, in insect cell-free translation system. J. Biosci. Bioeng. 102, 69–71.

Suzuki, T., Ito, M., Ezure, T., Shikata, M., Ando, E., Utsumi, T., Tsunasawa, S., Nishimura, O., 2006b. N-Terminal protein modifications in an insect cell-free protein synthesis system and their identification by mass spectrometry. Proteomics 6, 4486–4495.

Suzuki, T., Ito, M., Ezure, T., Shikata, M., Ando, E., Utsumi, T., Tsunasawa, S., Nishimura, O., 2007. Protein prenylation in an insect cell-free protein synthesis system and identification of products by mass spectrometry. Proteomics 7, 1942–1950.

Torres, A.S., Petri, V., Rae, T.D., O'Halloran, T.V., 2001. Copper stabilizes a heterodimer of the yCCS metallochaperone and its target superoxide dismutase. J. Biol. Chem. 276, 38410–38416.

Ukeda, H., Shimamura, T., Tsubouchi, M., Harada, Y., Nakai, Y., Sawamura, M., 2002. Spectrophotometric assay of superoxide anion formed in Maillard reaction based on highly water-soluble tetrazolium salt. Anal. Sci. 18, 1151–1154.

Yamaguchi, M., Nakazawa, T., Kuyama, H., Obama, T., Ando, E., Okamura, T.A., Ueyama, N., Norioka, S., 2005. High-throughput method for N-terminal sequencing of proteins by MALDI mass spectrometry. Anal. Chem. 77, 645–651.

Yamazaki, Y., Takao, T., 2008. Metalation states versus enzyme activities of Cu, Zn-superoxide dismutase probed by electrospray ionization mass spectrometry. Anal. Chem. 80, 8246–8252.

Journal of Biotechnology 145 (2010) 73–78

Contents lists available at ScienceDirect

Journal of Biotechnology

journal homepage: www.elsevier.com/locate/jbiotec

Preparation of ubiquitin-conjugated proteins using an insect cell-free protein synthesis system

Takashi Suzuki [a,*], Toru Ezure [a], Eiji Ando [a], Osamu Nishimura [b], Toshihiko Utsumi [c], Susumu Tsunasawa [b]

[a] Clinical and Biotechnology Business Unit, Life Science Business Department, Analytical and Measuring Instruments Division, Shimadzu Corporation, 1 Nishinokyo-Kuwabaracho, Nakagyo-ku, Kyoto 604-8511, Japan
[b] Institute for Protein Research, Osaka University, Osaka 565-0871, Japan
[c] Department of Biological Chemistry, Faculty of Agriculture, Yamaguchi University, Yamaguchi 753-8515, Japan

ARTICLE INFO

Article history:
Received 26 August 2009
Received in revised form 7 October 2009
Accepted 15 October 2009

Keywords:
Insect cell-free protein synthesis system
MALDI-TOF MS
Mdm2
p53
Ubiquitination

ABSTRACT

Ubiquitination is one of the most significant posttranslational modifications (PTMs). To evaluate the ability of an insect cell-free protein synthesis system to carry out ubiquitin (Ub) conjugation to *in vitro* translated proteins, poly-Ub chain formation was studied in an insect cell-free protein synthesis system. Poly-Ub was generated in the presence of Ub aldehyde (UA), a de-ubiquitinating enzyme inhibitor. *In vitro* ubiquitination of the p53 tumor suppressor protein was also analyzed, and p53 was poly-ubiquitinated when Ub, UA, and Mdm2, an E3 Ub ligase (E3) for p53, were added to the *in vitro* reaction mixture. These results suggest that the insect cell-free protein synthesis system contains enzymatic activities capable of carrying out ubiquitination. CBB-detectable ubiquitinated p53 was easily purified from the insect cell-free protein synthesis system, allowing analysis of the Ub-conjugated proteins by mass spectrometry (MS). Lys 305 of p53 was identified as one of the Ub acceptor sites using this strategy. Thus, we conclude that the insect cell-free protein synthesis system is a powerful tool for studying various PTMs of eukaryotic proteins including ubiqutination presented here.

1. Introduction

There is increasing interest in analyzing PTMs of proteins. Cell-free protein synthesis systems are potentially powerful tools for post-genomic studies including analyses of PTMs, because they can not only be used to synthesize desired proteins, including those toxic to cells (Sakurai et al., 2007), but they can also carry out various PTMs on these proteins. A cell-free protein synthesis system from *Spodoptera frugiperda* 21 (Sf21) insect cells (Ezure et al., 2006), which are widely used as the host for baculovirus expression systems, was developed previously, and it was demonstrated that this system could generate various eukaryotic-specific protein modifications, such as *N*-myristoylation (Suzuki et al., 2006b) and prenylation (Suzuki et al., 2007).

Ubiquitination is one of the most significant PTMs because it plays central roles in the regulation of many cellular processes, such as targeting for proteasome degradation, cell cycle progression, signal transduction, DNA repair, and so on (Ciechanover, 1998; Hershko and Ciechanover, 1998). Therefore, techniques to prepare Ub-conjugated proteins are extremely important to understand these processes in detail. Some methodologies for the purification of ubiquitinated proteins have been developed (Tomlinson et al., 2007), and large-scale MS analyses have been performed (Peng et al., 2003; Gururaja et al., 2003). However, it is still challenging to identify ubiquitinated proteins and Ub-conjugation sites.

A rabbit reticulocyte lysate system has often been utilized for *in vitro* ubiquitination assays of target proteins, because it possesses enzymatic activities involved in the ubiquitination reaction (Ciechanover et al., 1991; Etlinger and Goldberg, 1977). However, a serious drawback of this system is that only radio-isotope labeling or an immunoblotting strategy may be used to detect ubiquitinated proteins, because of the low expression levels.

In order to evaluate whether the insect cell-free protein synthesis system contains enzymes capable of carrying out ubiquitination reactions, poly-Ub chain formation was investigated using the insect cell-free protein synthesis system and FLAG-tagged Ub. The p53 tumor suppresor protein was chosen as a model protein because it is highly regulated by the ubiquitin–proteasome pathway (Haupt et al., 1997), and *in vitro* ubiquitination of p53 occurred.

Abbreviations: PTMs, posttranslational modifications; Ub, ubiquitin; UA, ubiquitin aldehyde; E3, E3 ubiquitin ligase; MS, mass spectrometry; Sf21, *Spodoptera frugiperda* 21; Me-Ub, methylated ubiquitin; MALDI-TOF MS, matrix assisted laser desorption/ionization time-of-flight mass spectrometry; QIT, quadrupole ion trap; MS/MS, tandem mass spectrometry; *m/z*, mass-to-charge ratio.

* Corresponding author. Tel.: +81 75 823 1351; fax: +81 75 823 1364.
E-mail address: t-suzuki@shimadzu.co.jp (T. Suzuki).

0168-1656/$ – see front matter © 2009 Elsevier B.V. All rights reserved.
doi:10.1016/j.jbiotec.2009.10.009

The present study describes a simple and robust strategy to prepare ubiquitin-conjugated proteins using this cell-free protein synthesis system and the identification of exact location of Ub-conjugation sites by mass spectrometry.

2. Materials and methods

2.1. Materials

Transdirect *insect cell*, which is based on the Sf21 extract, is a commercial product of Shimadzu (Kyoto, Japan). Restriction endonucleases and DNA modifying enzymes were purchased from Toyobo (Osaka, Japan) and New England Biolabs (Ipswich, MA, USA). Human cDNA clone p53 (GenBank accession no. **NM_000546**) and Mdm2 (GenBank accession no. **BT007258**) were obtained from Toyobo and Open Biosystems (Huntsville, AL, USA), respectively. Caspase-3 Inhibitor I (Ac-DEVD-CHO) and MG-132 (Z-LLL-CHO) were obtained from Calbiochem (Darmstadt, Germany). Ubiquitin and FLAG-tagged ubiquitin were purchased from Sigma (St. Louis, MO, USA). Ubiquitin aldehyde and methylated ubiquitin were obtained from Peptide Institute (Osaka, Japan) and BostonBiochem (Cambridge, MA, USA), respectively.

2.2. Construction of expression clones for in vitro translation

The protein coding regions of human p53 were amplified by PCR and inserted into the multiple cloning site of the pTD1-strep vector, which is an expression vector for synthesizing C-terminal *Strep*-tagged target proteins using the insect cell-free protein synthesis system (Ezure et al., 2007). The resultant plasmid was named pTD1-strep-p53. The ORF of the human Mdm2 gene was amplified by PCR. The amplified DNA fragment was ligated into the pTD1-vector (Suzuki et al., 2006a), and the resulting plasmid was designated pTD1-Mdm2. N-terminal or C-terminal GST-tagged Mdm2 constructs were also constructed using conventional cloning techniques. The resultant plasmids were named pTD1-NGST-Mdm2 and pTD1-CGST-Mdm2, respectively. The DNA sequences of these recombinant constructs were confirmed by the dideoxynucleotide chain termination method.

2.3. In vitro transcription and translation

mRNAs were synthesized with the T7 RiboMAX Express Large Scale RNA Production System (Promega, Madison, WI, USA) using linearized expression clones as the template. Purification of *in vitro* transcribed mRNAs was performed as described previously (Suzuki et al., 2006b). *In vitro* translation was carried out using an insect cell-free protein synthesis system according to the instruction manual. In the case of Mdm2, translation was performed with or without the addition of a caspase-3 inhibitor I at a final concentration of 1.0 μM.

2.4. Detection of synthesized proteins by fluorescent labeling

For the synthesis of fluorescently labeled proteins, 1 μL of FluoroTect $Green_{Lys}$ tRNA (Promega) was added to 50 μL of the *in vitro* translation reaction mixture. The sample was resolved by SDS-PAGE. The fluorescently labeled proteins were detected using a laser-based fluorescent scanner, Molecular Imager FX (Bio-Rad Laboratories, Hercules, CA, USA).

2.5. Poly-Ub chain formation

The Sf21 cell-free extract for the insect cell-free protein synthesis system (75 μL) and the N-terminal FLAG-tagged Ub (50 μg) were mixed and incubated at 25 °C for 2 h in a 250 μL reaction mixture that included ubiquitination buffer (50 mM Tris–HCl, pH 7.5, containing 5 mM $MgCl_2$, 1 mM ATP, 10 mM creatine phosphate, 4 U mL^{-1} creatine kinase and 2.5 mM dithiothreitol) and 5 μg of ubiquitin aldehyde (UA).

2.6. In vitro ubiquitination assay

In vitro translated p53 (6 μL) and Mdm2 (4 μL) were mixed and incubated at 30 °C for 2 h in a 25 μL reaction mixture that included the ubiquitination buffer, 0.63 μg of UA, and 6.3 μg of Ub. Methylated Ub (Me-Ub) was added instead of Ub to the *in vitro* ubiquitination reaction mixture to suppress poly-Ub chain formation.

2.7. Affinity purification

Affinity purification of FLAG-tagged or strep-tagged proteins was performed as described previously (Suzuki et al., 2006b, 2007). In the case of GST-tagged proteins, a GST purification module was used (GE Healthcare, Piscataway, USA).

2.8. Analysis of N-terminal amino acid sequence

The affinity-purified protein was separated by SDS-PAGE and then transferred to a PVDF membrane, then stained with CBB R-250. The protein band was sequenced with a PPSQ-33A protein sequencer (Shimadzu).

2.9. Mass spectrometry

The tryptic digests from affinity-purified proteins were analyzed with an AXIMA-CFR-plus MALDI-TOF MS (matrix assisted laser desorption/ionization time-of-flight mass spectrometry) instrument and an AXIMA-QIT MALDI-QIT (quadrupole IT)-TOF hybrid mass spectrometer (Shimadzu/Kratos, Manchester, UK) as described previously (Suzuki et al., 2006b).

3. Results

3.1. Poly-Ub chain formation using the insect cell-free extract

To evaluate the ability of the insect cell-free protein synthesis system to conjugate Ub to target proteins synthesized *in vitro*, generation of poly-Ub chains was analyzed after adding Ub to the cell-free extract of the insect cell-free protein synthesis system. FLAG-tagged Ub and the extract were incubated in the ubiquitination buffer, and then FLAG-tagged Ub was collected by affinity purification. The reaction was performed in the presence or absence of UA, a de-ubiquitinating enzyme inhibitor. Ladder bands at around 15–27 kDa, which probably corresponded to poly-Ubs, were observed upon SDS-PAGE of the affinity-purified sample after UA was added to the reaction mixture (Fig. 1). A protein band detected around 50 kDa was identified as β-tubulin by peptide mass fingerprinting (data not shown). This is probably a non-specific protein band because β-tubulin has been sometimes coeluted in the affinity purification step (Suzuki et al., 2007). On the other hand, when the reaction was carried out without adding UA, only a predominant 10 kDa band was detected (Fig. 1). The 10 kDa band and slowly migrating bands were excised individually and digested with trypsin, and the digests were analyzed by MALDI-TOF MS. The spectra produced from these samples were almost identical, and these MS spectra corresponded to tryptic digests of Ub (Fig. 2). Trypsin digestion of ubiquitinated proteins produces peptides with internal lysine residues harboring a di-glycine remnant (GG-tag)

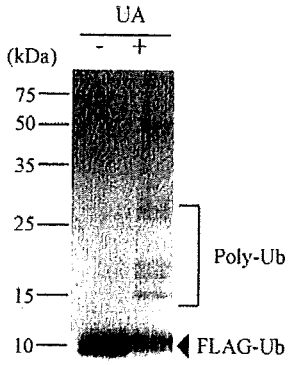

Fig. 1. Poly-Ub chain formation in the insect cell-free protein synthesis system. N-terminal FLAG-tagged Ub (50 μg) was added to the insect cell-free extract and incubated in the presence or absence of UA. After the incubation, FLAG-tagged Ub was purified as reported previously (Suzuki et al., 2007). The affinity eluate was concentrated to about 25 μL by ultrafiltration (molecular cutoff = 3 kDa). Five microliters of the concentrate was electrophoresed on a 15% SDS-PAGE gel and visualized by CBB staining.

derived from the C-terminus of Ub (Peng et al., 2003). Therefore, a search for ions corresponding to the tryptic peptide having a GG-tag was performed. Specific peaks that probably included a GG-tag were observed at *m/z* (mass-to-charge ratio) 1460.72, 1836.93, and 2244.09 in the MS spectra of tryptic digests of ladder bands (Fig. 2a). These ions were further subjected to tandem MS (MS/MS) analysis and identified as tryptic fragments of Ub containing a GG-tag on Lys 48, Lys 29, and Lys 63, respectively (Fig. 3), suggesting that the insect cell-free protein synthesis system contains enzymatic activities capable of carrying out ubiquitination and de-ubiquitination.

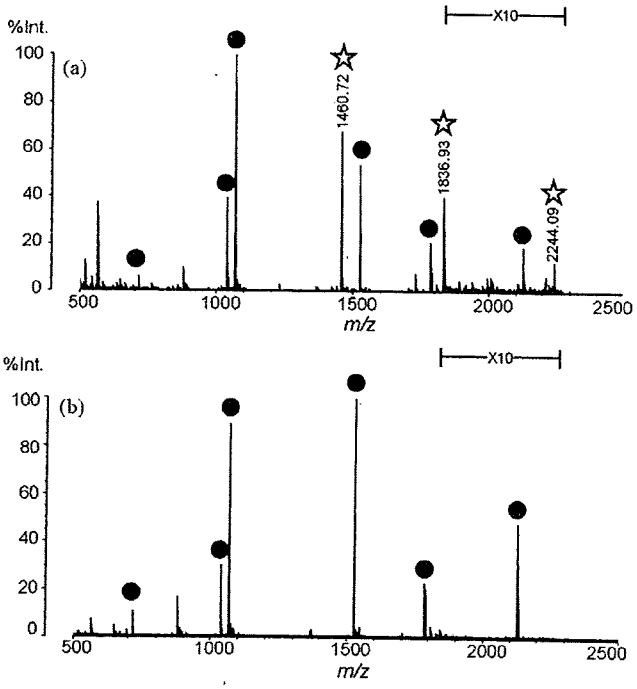

Fig. 2. MALDI-mass spectra of tryptic digests of the affinity-purified Ubs. The protein bands corresponding to (a) slowly migrating bands (around 15–27 kDa) and (b) 10 kDa were excised individually and digested with trypsin, and each digest was analyzed by MALDI-TOF MS. Filled circles indicate ions with the theoretical *m/z* values of tryptic digests of Ub. Stars indicate probable tryptic peptides containing a GG-tag.

3.2. *In vitro* ubiquitination of the p53 tumor suppressor using the insect cell-free protein synthesis system

To investigate whether the insect cell-free protein synthesis system has the ability to conjugate Ub to target proteins, the p53 tumor suppressor was chosen as a model protein. *In vitro* translation of mRNA encoding this protein was performed, and the *in vitro* ubiquitination assay was carried out as described in Section 2. A slight protein band probably corresponding to mono-ubiquitinated p53 was generated upon addition of both Ub and UA (Fig. 4: lane 4). To increase the efficiency of the p53 Ub-conjugation reaction, cell-free synthesized Mdm2, an E3 Ub ligase (E3) for p53 (Fang et al., 2000), was added to the *in vitro* ubiquitination reaction mixture. However, this produced no measurable effect (Fig. 4: lane 5).

To solve this problem, the *in vitro* synthesized Mdm2 was analyzed more closely, and it was noted that translation of the Mdm2 gene unexpectedly generated a 60 kDa protein band (Fig. 5), although the full-length predicted gene product of Mdm2 was

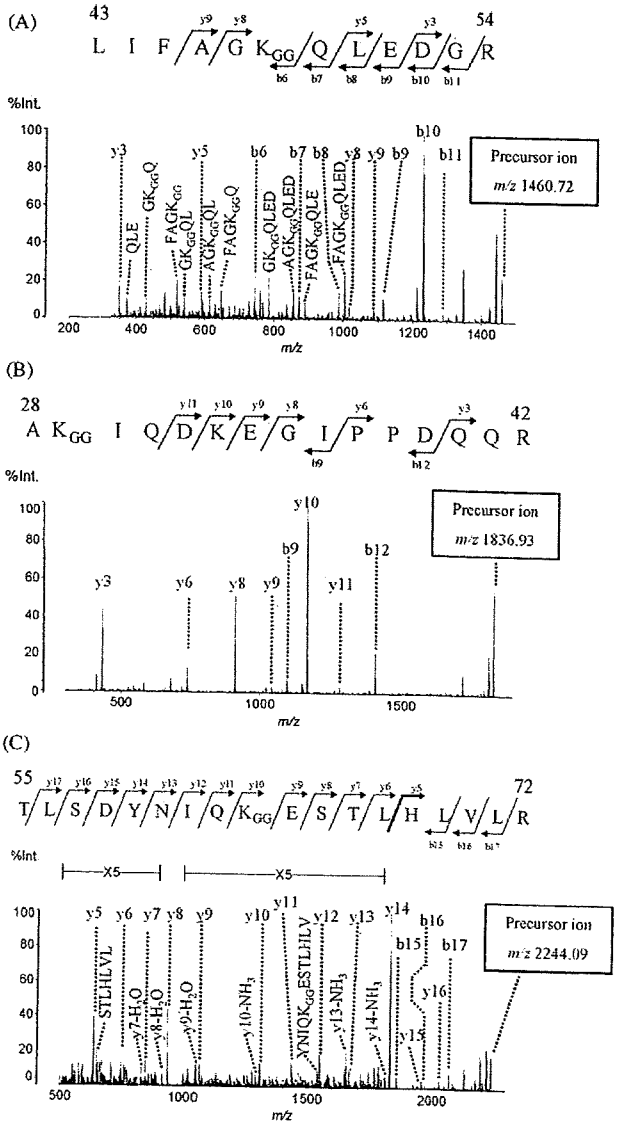

Fig. 3. MALDI-MS/MS spectra of the tryptic peptides containing a GG-tag derived from poly-Ub. MS/MS analyses were performed for the ions detected at *m/z* 1460.72 (A), *m/z* 1836.93 (B), and *m/z* 2244.09 (C) in the mass spectra of the tryptic digests from poly-Ub. The observed fragment ions are indicated by the sequences shown. The subscript "GG" represents di-glycine residues from the C-terminal region of Ub.

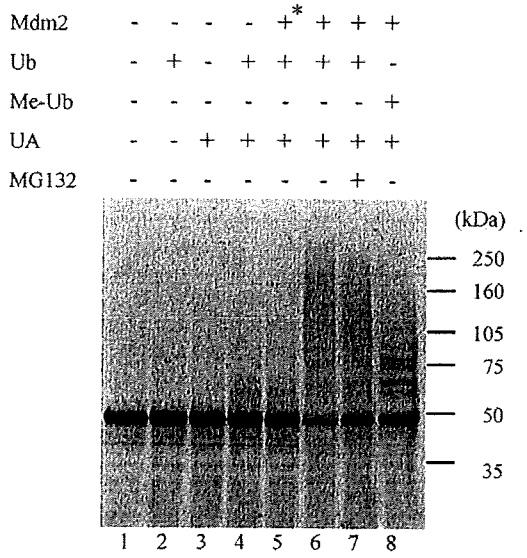

Fig. 4. *In vitro* ubiquitination of p53 using the insect cell-free protein synthesis system. Six microliters of *in vitro* translated and fluorescently labeled p53 was mixed with 4 μL of Mdm2 translated in the presence of the caspase-3 inhibitor (Ac-DEVD-CHO). *In vitro* ubiquitination assays were performed by adding Ub/Me-Ub and UA as described in Section 2. After the incubation, the total volume of the mixture was electrophoresed on a 5–20% SDS-PAGE gel. Asterisk indicates *in vitro* translated Mdm2 in the absence of the caspase-3 inhibitor.

reported to be a protein with molecular weight of about 100 kDa (Pochampally et al., 1998). This result suggested that the Mdm2 gene product was cleaved by a protease(s) in the insect cell-free protein synthesis system. To investigate this possibility further, N-terminal and C-terminal GST-tagged Mdm2 plasmids were constructed. Expression analyses of these constructs suggested that the cleavage site of the synthesized Mdm2 was located in the C-terminal region of the full-length Mdm2 protein (data not shown). The N-terminal amino acid sequence of the affinity-purified, C-terminal GST-tagged Mdm2 was NH_2-^{362}XKKTIVNPSR^{371} (data not shown). Therefore, a mutant Mdm2 construct was generated with an Ala substitution of Asp 361, and this protein escaped proteolytic degradation by an Mdm2-cleaving enzyme (data not shown). These results indicate the cleavage site of the cell-free synthesized Mdm2 is between Asp 361 and Cys 362. It has been reported that Mdm2 is cleaved by caspase-3 at the C-terminal side of the Asp 361 residue (Chen et al., 1997). Therefore, the effect of adding a caspase inhibitor on the translation product of Mdm2 was evaluated. The Mdm2-cleaving enzyme activity was almost completely inhibited by addition of the caspase-3 inhibitor (Ac-DEVD-CHO) (Fig. 5), suggesting that a caspase-like activity exists in the insect cell-free protein synthesis system.

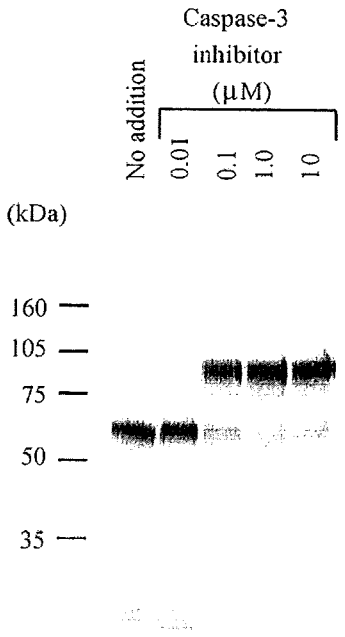

Fig. 5. A caspase-like activity in the insect cell-free protein synthesis system and its inhibition by a caspase-3 inhibitor. Fluorescent labeling of *in vitro* translated Mdm2 protein was carried out using FluoroTect as described in Section 2. Translation was performed in the presence or absence of a caspase-3 inhibitor I (Ac-DEVD-CHO). After the translation, 6 μL of the reaction mixture was electrophoresed on a 10% SDS-PAGE gel.

It has been reported that cleavage after Asp 361 by an Mdm2-specific caspase divides Mdm2 into an N-terminal fragment that binds p53 and a C-terminal RING-finger domain, resulting in loss of its E3 activity (Pochampally et al., 1999). Therefore it is likely that the inefficient Ub conjugation to p53 in the insect cell-free protein synthesis system was also owing to loss of the E3 activity of Mdm2 in this *in vitro* system. *In vitro* ubiquitination of p53 was next attempted in the insect cell-free protein synthesis system in the presence of the caspase-3 inhibitor Ac-DEVD-CHO, resulting in a remarkable acceleration of Ub conjugation to p53, presumably due to the concomitant production of full-length Mdm2 (Fig. 4: lane 6).

Mdm2-mediated ubiquitination drives p53 to proteasomal degradation (Rodriguez et al., 2000). To investigate whether the insect cell-free protein synthesis system has proteasomal activity, a proteasome inhibitor, MG132, was added to the *in vitro* ubiquitination reaction mixture. However, the addition of MG132 to the insect cell-free protein synthesis system produced only a slight effect (Fig. 4: lane 7). The addition of lactacystin, a specific proteasome inhibitor, also showed no effect on the mobility pattern of p53 on SDS-PAGE (data not shown). Further studies are necessary to clarify this finding.

It has been reported that Mdm2 mediates multiple mono-ubiquitinations of p53 (Lai et al., 2001). Therefore the ubiquitination reaction was performed using Me-Ub to investigate whether the type of ubiquitination generated in the insect cell-free protein synthesis system is mono- or poly-ubiquitination. Ladder bands at around 60–100 kDa were remarkably enhanced in the ubiquitination assay using Me-Ub (Fig. 4: lane 8). This result suggested that poly-ubiquitination of p53 occurred when Ub, UA, and full-length Mdm2 were added to the *in vitro* ubiquitination reaction carried out by the insect cell-free protein synthesis system.

3.3. Affinity purification of in vitro ubiquitinated p53

To evaluate the performance of insect cell-free protein synthesis system as a tool for production of Ub-conjugated proteins, *in vitro* ubiquitination of p53 was carried out using Me-Ub at a 2.5 mL reaction scale. The *in vitro* synthesized and ubiquitinated p53 was collected by affinity purification, and CBB-detectable ubiquitinated p53 proteins were thus obtained (Fig. 6). This result suggests that the insect cell-free protein synthesis system is an effective tool to prepare ubiquitinated proteins of interest.

3.4. Mass spectrometric analyses of in vitro ubiquitinated p53

The 50 kDa and ladder bands were excised individually and digested with trypsin, and these tryptic digests were analyzed by MALDI-TOF MS. Peaks detected in the mass spectrum of the tryptic digests of the 50 kDa band agreed well with the theoretical *m/z* values for the p53 protein (about 67% sequence coverage, Fig. 7A-b). The MALDI-mass spectra produced from each of the ladder

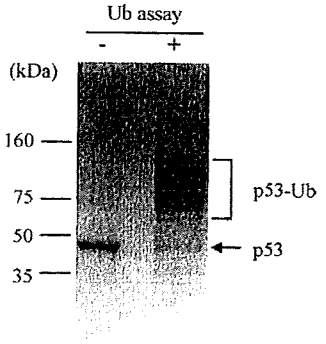

Fig. 6. SDS-PAGE of the affinity-purified p53 proteins. An *in vitro* ubiquitination reaction was carried out using Me-Ub at a 2.5 mL reaction scale. Ubiquitinated p53 was collected by affinity purification and concentrated to about 20 μL by ultrafiltration (molecular cutoff = 10 kDa). Eight microliters of the concentrate was electrophoresed on 10% SDS-PAGE and visualized by CBB staining.

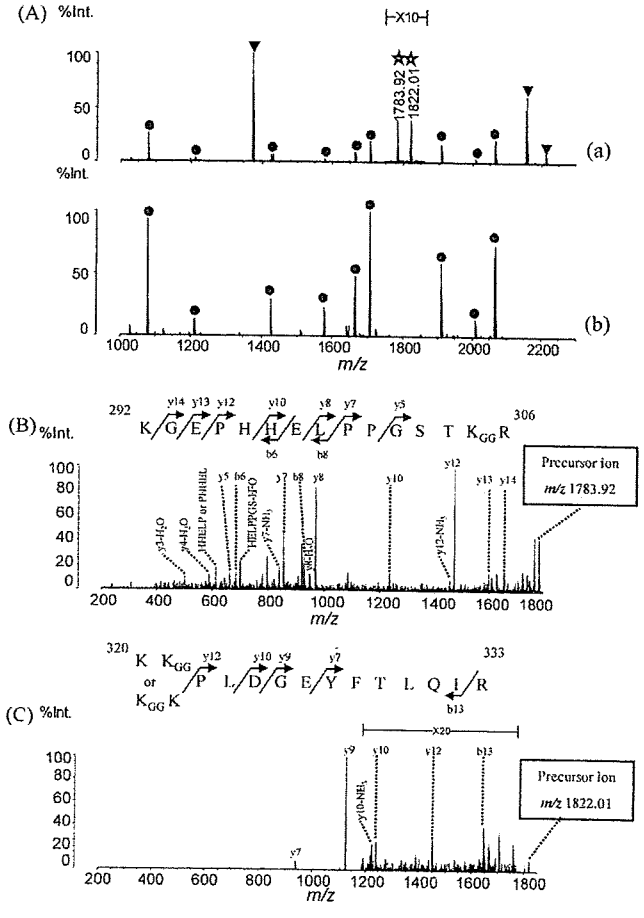

Fig. 7. MALDI-mass and -MS/MS spectra of tryptic digests of the affinity-purified p53 proteins. (A) The protein bands corresponding to (a) ubiquitinated p53 (p53-Ub) and (b) p53 proteins were excised individually. Each protein band was reduced and *S*-alkylated with iodeacetamide and then digested overnight with trypsin, and the digests were analyzed by MALDI-TOF MS. Filled circles and triangles indicate ions with the theoretical *m/z* values of tryptic digests of p53 and Me-Ub, respectively. Stars indicate probable tryptic peptides containing a GG-tag. MS/MS analyses were performed for the ions detected at *m/z* 1783.92 (B) and *m/z* 1822.01 (C) in (A). The observed fragment ions are indicated by the sequences shown. The subscript "GG" represents di-glycine residues from the C-terminal region of Ub.

bands were almost identical (A typical result is shown in Fig. 7A-a.). Peaks corresponding to tryptic peptides from both p53 and Me-Ub were detected in the mass spectrum (Fig. 7A-a). This result clearly indicated that Ub conjugation to p53 was generated in the insect cell-free protein synthesis system. The high molecular weight band (>160 kDa) detected in Fig. 6 was also analyzed by peptide mass fingerprinting, but we could not identify it (data not shown).

To identify the Ub-conjugation sites on p53, peaks corresponding to the tryptic digests were searched to find peptides with a GG-tag. Two peaks from the tryptic digests containing a GG-tag were detected at *m/z* 1783.92 and 1822.01 (Fig. 7A-a). These ions were further analyzed by MS/MS, which indicated that these ions were tryptic peptides having a GG-tag at Lys 305 (*m/z* 1783.92) and at Lys 320/321 (*m/z* 1822.01) (Fig. 7B and C).

4. Discussion

Ubiquitination is widely carried out in various cellular processes. Conjugation of Ub to target proteins can occur in both monomeric (mono-ubiquitination) and polymeric (poly-ubiquitination) forms. All seven internal Lys residues of Ub (Lys 6, 11, 27, 29, 33, 48, and 63) can be conjugated to Ub moieties to form poly-Ub chains (Ikeda and Dikic, 2008). In this study, we confirmed by MALDI-TOF MS and MALDI-QIT-TOF MS that Lys 29-, Lys 48-, and Lys 63-linked poly-Ub chain formation occurred in an insect cell-free protein synthesis system. Although it is unclear whether poly-Ub chains linked to other Lys residues are generated, and how many kinds of E2 Ub-conjugating enzymes and E3s exist in the insect cell-free protein synthesis system, the present results are sufficiently convincing to conclude that the insect cell-free protein synthesis system contains enzymatic activities capable of carrying out ubiquitination.

It is well accepted that ubiquitination plays a major role in p53 regulation. Although the C-terminal Lys residues (Lys 370, 372, 373, 381, 382, and 386) of p53 are known to be the major Ub acceptor sites for Mdm2-mediated ubiquitination (Rodriguez et al., 2000; Nakamura et al., 2000), the exact locations of the actual Ub acceptor sites of p53 are not fully defined. Although the possibility cannot be excluded that the Ub acceptor sites identified in this study may not accurately reflect the *in vivo* situation, we demonstrated that Lys 305 of p53 was one Ub acceptor site (Fig. 7B and Fig. 8). On the other hand, major Ub acceptor sites mediated by Mdm2 were not detected by MS analyses (Fig. 8), although Ub conjugations to p53 in the insect cell-free protein synthesis system were accelerated in the presence of Mdm2. One possible explanation for this is that it may be difficult to detect tryptic peptides from the C-terminal region of p53 by MALDI-TOF MS, because many short tryptic peptides are produced due to the existence of numerous Lys and Arg residues in this region (Fig. 8). It is not clear from the obtained results whether the Ub conjugations at Lys 305 and Lys 320/321 of p53 were mediated by Mdm2 or by another E3 in the insect cell-free protein synthesis system. The latter alternative is thought to be possible for the following reasons. First, it was recently demonstrated that E4F1, which is a zinc-finger protein, stimulates p53 ubiquitination on Lys 319 to Lys 321, and it was also demonstrated that these acceptor lysines are distinct from those targeted by Mdm2 (Cam et al., 2006) (Fig. 8). Second, Ub conjugation to p53 in the insect cell-free protein synthesis system was observed in the absence of Mdm2 (Fig. 4: lane 4).

We emphasize that Ub-conjugated p53 proteins were easily obtained using the insect cell-free protein synthesis system from the mRNA template transcribed from the corresponding cDNA. Thus this strategy should also be applicable to other cDNA resources. Although it is desirable that Ub conjugations occur effectively on target proteins without the addition of an exogenous

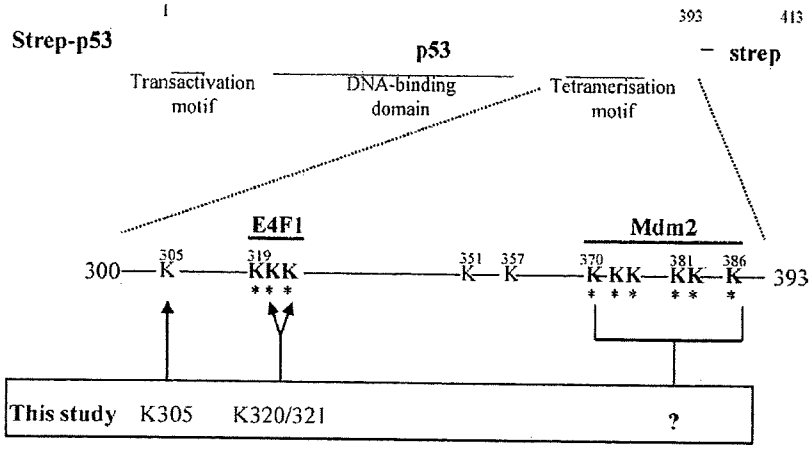

Fig. 8. Schematic representation of ubiquitination sites of p53. Asterisks indicate ubiquitination sites identified previously (Rodriguez et al., 2000; Nakamura et al., 2000; Cam et al., 2006). Arrows indicate Ub acceptor lysines determined in this study.

E3 protein, we think that it might be difficult because many E3s are tightly regulated by Ub-proteasome pathway or other PTMs (Meek and Knippschild, 2003). Further studies are necessary to elucidate general applicability of the insect cell-free protein synthesis system for *in vitro* ubiquitination assays. Quite recently, a method for *in vitro* analysis of ubiquitination based on wheat germ cell-free protein synthesis system and liminescent detection was reported (Takahashi et al., 2009). Although this strategy is effective for high-throughout detection of ubiquitination, it cannot be used to identify the exact location of the modification. We demonstrated that the ubiquitination sites generated *in vitro* could be identified by using the insect cell-free protein synthesis system and mass spectrometry. We think that it is critical to identify the precise structure and the exact location of the modification in PTM analysis. Thus, this insect cell-free protein synthesis system should prove to be a potent tool for *in vitro* ubiquitination assays of target proteins.

Acknowledgement

We thank Dr. Minoru Yamaguchi, Shimadzu Corporation, for the analysis of N-terminal amino acid sequences.

References

Cam, L.L., Linares, L.K., Paul, C., Julien, E., Lacroix, M., Hatchi, E., Triboulet, R., Bossis, G., Shmueli, A., Rodriguez, M.S., Coux, O., Sardet, C., 2006. E4F1 is an atypical ubiquitin ligase that modulates p53 effector functions independently of degradation. Cell 127, 775–788.

Chen, L., Marechal, V., Moreau, J., Levine, A.J., Chen, J., 1997. Proteolytic cleavage of the mdm2 oncoprotein during apoptosis. J. Biol. Chem. 272, 22966–22973.

Ciechanover, A., Digiuseppe, J.A., Bercovich, B., Orian, A., Richter, J.D., Schwartz, A.L., Brodeur, G.M., 1991. Degradation of nuclear oncoproteins by the ubiquitin system *in vitro*. Proc. Natl. Acad. Sci. U.S.A. 88, 139–143.

Ciechanover, A., 1998. The ubiquitin–proteasome pathway: on protein death and cell life. EMBO J. 17, 7151–7160.

Etlinger, J.D., Goldberg, A.L., 1977. A soluble ATP-dependent proteolysis system responsible for the degradation of abnormal proteins in reticulocytes. Proc. Natl. Acad. Sci. U.S.A. 74, 54–58.

Ezure, T., Suzuki, T., Higashide, S., Shintani, E., Endo, K., Kobayashi, S., Shikata, M., Ito, M., Tanimizu, K., Nishimura, O., 2006. Cell-free protein synthesis system prepared from insect cells by freeze–thawing. Biotechnol. Prog. 22, 1570–1577.

Ezure, T., Suzuki, T., Shikata, M., Ito, M., Ando, E., Nishimura, O., Tsunasawa, S., 2007. Expression of proteins containing disulfide bonds in an insect cell-free system and confirmation of their arrangements by MALDI-TOF mass spectrometry. Proteomics 7, 4424–4434.

Fang, S., Jensen, J.P., Ludwig, R.L., Vousden, K.H., Weissman, A.M., 2000. Mdm2 is a RING finger-dependent ubiquitin protein ligase for itself and p53. J. Biol. Chem. 275, 8945–8951.

Gururaja, T., Li, W., Noble, W.S., Payan, D.G., Anderson, D.C., 2003. Multiple functional categories of proteins identified in an in vitro cellular ubiquitin affinity extract using shotgun peptide sequencing. J. Proteome Res. 2, 394–404.

Haupt, Y., Maya, R., Kazaz, A., Oren, M., 1997. Mdm2 promotes the rapid degradation of p53. Nature 387, 296–299.

Hershko, A., Ciechanover, A., 1998. The ubiquitin system. Annu. Rev. Biochem. 67, 425–479.

Ikeda, F., Dikic, I., 2008. Atypical ubiquitin chains: new molecular signals. EMBO Rep. 9, 536–542.

Lai, Z., Ferry, K.V., Diamond, M.A., Wee, K.E., Kim, Y.B., Ma, J., Yang, T., Benfield, P.A., Copeland, R.A., Auger, K.R., 2001. Human mdm2 mediates multiple monoubiquitination of p53 by a mechanism requiring enzyme isomerization. J. Biol. Chem. 276, 31357–31367.

Meek, D.W., Knippschild, U., 2003. Posttranslational modification of MDM2. Mol. Cancer Res. 1, 1017–1026.

Nakamura, S., Roth, J.A., Mukhopadhyay, T., 2000. Multiple lysine mutations in the C-terminal domain of p53 interfere with Mdm2-dependent protein degradation and ubiquitination. Mol. Cell. Biol. 20, 9391–9398.

Peng, J., Schwartz, D., Elias, J.E., Thoreen, C.C., Cheng, D., Marsischky, G., Roelofs, J., Finley, D., Gygi, S.P., 2003. A proteomics approach to understanding protein ubiquitination. Nat. Biotechnol. 21, 921–926.

Pochampally, R., Fodera, B., Chen, L., Shao, W., Levine, E.A., Chen, A., 1998. A 60 kd MDM2 isoform is produced by caspase cleavage in non-apoptotic tumor cells. Oncogene 17, 2629–2636.

Pochampally, R., Fodera, B., Chen, L., Lu, W., Chen, J., 1999. Activation of an MDM2-specific caspase by p53 in the absence of apoptosis. J. Biol. Chem. 274, 15271–15277.

Rodriguez, M.S., Desterro, J.M.P., Lain, S., Lane, D.P., Hay, R.T., 2000. Multiple C-terminal lysine residues target p53 for ubiquitin-proteasome-mediated degradation. Mol. Cell. Biol. 20, 8458–8467.

Sakurai, N., Moriya, K., Suzuki, T., Sofuku, K., Mochiki, H., Nishimura, O., Utsumi, T., 2007. Detection of co- and post-translational protein N-myristoylation by metabolic labeling in an insect cell-free protein synthesis system. Anal. Biochem. 362, 236–244.

Suzuki, T., Ito, M., Ezure, T., Kobayashi, S., Shikata, M., Tanimizu, K., Nishimura, O., 2006a. Performance of expression vector, pTD1, in insect cell-free translation system. J. Biosci. Bioeng. 102, 69–71.

Suzuki, T., Ito, M., Ezure, T., Shikata, M., Ando, E., Utsumi, T., Tsunasawa, S., Nishimura, O., 2006b. N-Terminal protein modifications in an insect cell-free protein synthesis system and their identification by mass spectrometry. Proteomics 6, 4486–4495.

Suzuki, T., Ito, M., Ezure, T., Shikata, M., Ando, E., Utsumi, T., Tsunasawa, S., Nishimura, O., 2007. Protein prenylation in an insect cell-free protein synthesis system and identification of products by mass spectrometry. Proteomics 7, 1942–1950.

Takahashi, H., Nozawa, A., Seki, M., Shinozaki, K., Endo, Y., Sawasaki, T., 2009. A simple and high-sensitivity method for analysis of ubiquitination and polyubiquitination based on wheat cell-free protein synthesis. BMC Plant Biol. 9, 39.

Tomlinson, E., Palaniyappan, N., Tooth, D., Layfield, R., 2007. Methods for the purification of ubiquitinated proteins. Proteomics 7, 1016–1022.

Acta histochemica ▮ (▮▮▮▮) ▮▮▮–▮▮▮

ELSEVIER

Available online at www.sciencedirect.com

ScienceDirect

acta histochemica

www.elsevier.de/acthis

Molecular-assisted immunohistochemical optimization

Mohd Feroz Mohd Omar[a,b], Ning Huang[c,d], Keli Ou[c,d], Kun Yu[e], Thomas C. Putti[f], Hiroyuki Jikuya[c,d], Tetsuo Ichikawa[c,d], Osamu Nishimura[g], Patrick Tan[c,e,h,i], Manuel Salto-Tellez[a,f,*]

[a]*Oncology Research Institute, National University of Singapore, Singapore*
[b]*NUS Graduate School for Integrative Sciences and Engineering, Singapore*
[c]*Agenica Research Pte Ltd., Singapore*
[d]*Shimadzu (Asia Pacific) Pte Ltd., Singapore*
[e]*National Cancer Centre of Singapore, Singapore*
[f]*Department of Pathology, National University Hospital and National University of Singapore, 5, Lower Kent Ridge Road, 119074, Singapore*
[g]*Shimadzu Corporation, Nakagyo-ku, Kyoto, Japan*
[h]*Genome Institute of Singapore, Singapore*
[i]*Duke-NUS Graduate Medical School, Singapore*

Received 19 August 2008; received in revised form 6 May 2009; accepted 19 May 2009

KEYWORDS
Immunohistochemistry validation;
Molecular biology;
Molecular diagnostics;
Protein immunolocalization;
Antibody optimization

Summary

Immunohistochemistry (IHC) is an essential tool in diagnostic surgical pathology, allowing analysis of protein subcellular localization. The use of IHC by different laboratories has lead to inconsistencies in published literature for several antibodies, due to either interpretative (inter-observer variation) or technical reasons. These disparities have major implications in both clinical and research settings. In this study, we report our experience conducting an IHC optimization of antibodies against five proteins previously identified by proteomic analysis to be breast cancer biomarkers, namely 6PGL (PGLS), CAZ2 (CAPZA2), PA2G4 (EBP1) PSD2 and TKT. Large variations in the immunolocalizations and intensities were observed when manipulating the antigen retrieval method and primary antibody incubation concentration. However, the use of an independent molecular analysis method provided a clear indication in choosing the appropriate biologically and functionally relevant "staining pattern". Without this latter step, each of these contradictory results would have been *a priori* "technically acceptable" and would have led to different biological and functional interpretations of these proteins and potentially

*Corresponding author at: Department of Pathology, National University Hospital and National University of Singapore, 5, Lower Kent Ridge Road, 119074, Singapore. Tel.: +65 67724704; fax: +65 6778 0671.
E-mail address: patmst@nus.edu.sg (M. Salto-Tellez).

0065-1281/$ - see front matter
doi:10.1016/j.acthis.2009.05.010

Please cite this article as: Mohd Omar MF, et al. Molecular-assisted immunohistochemical optimization. Acta Histochem (2009), doi:10.1016/j.acthis.2009.05.010

different applications in a routine pathology setting. Thus, we conclude that full validation of immunohistochemical protocols for scientific and clinical use will require the incorporation of biological knowledge of the biomarker and the disease in question.

Introduction

Protein expression is the true "functional genomics" and knowledge of extracellular and/or subcellular localization is essential to elucidate the function of these proteins. Measuring the levels of protein expression and their putative correlation with RNA through gene expression are common activities in modern translational research. In the diagnostic arena, the use of immunohistochemistry (IHC) in addition to hematoxylin and eosin staining has been shown to increase diagnostic accuracy. Insights into the role of protein expression in disease progression and how this affects patient stratification and drug targeting, will ultimately lead to formulating the basis for personalized medicine (Douglas-Jones et al., 2005). The availability of tissues and the relative simplicity of IHC techniques make this a very widely used and accepted method for routine diagnostics.

IHC allows the *in situ* visualization of protein localization in specific cellular components, not only in the different regions of the tissue, but also within specific regions of cells. This is achieved by the precise interaction of an introduced antibody with a specific antigen, later visualized using a labelling system. For the most part, this technique is semi-quantitative and predominantly analyzed by a trained pathologist. Technically simple and relatively affordable, IHC is arguably the most widely used "molecular" analysis in research and diagnostic settings. Unfortunately, the wide use of this technique, which allows an "interpretative" approach to the analysis of results, also accounts for the known reported disparities in the results.

These disparities have been reported with regard to key molecular players in common cancers such as p53 in colorectal cancer (Soong et al., 1996) and estrogen receptor and c-erbB2 in breast cancer (Nedergaard et al., 1995; Perez et al., 2006) among many others which, in the case of breast cancer, may lead to suboptimal patient treatment. These apparent contradictions can be interpretative or technical. Classically, IHC interpretation is subjective (Biesterfeld et al., 1996), leading to inter-observer variability, which results in different observers scoring a particular case differently. Although systems for automated scoring of IHC are already commercially available, (Rojo et al., 2006) and some of them approved by the US Food and Drug Administration (FDA) for quantification of specific antibodies, these are not yet ready for universal use in research or diagnosis. Technical disparities are primarily attributed to differences in fixation protocol, IHC reagents, antigen retrieval protocols, antibody clone, concentrations and incubation times (Ainsworth et al., 2005; Boenisch, 2005; Goldstein et al., 2007; McCabe et al., 2005; McShane et al., 2000; Press et al., 1994, 2002; Ramos-Vara, 2005; Shi et al., 1997, 2001). These inconsistencies are a major hindrance in both clinical and research areas as they impact the interpretation of critical factors including clinical outcome, prognosis and potential biomarker discovery.

When working with a previously untested antibody, optimum experimental conditions must be established. To do so, several protocols are attempted to obtain 'correct' results based on the subjective criteria set by the researcher, such as immunolabelling intensity and absence of background 'noise'. This is, by definition, an arbitrary exercise, which may result in inter-observer variability. One approach to overcome this would be to introduce a 'standard' with which the immunolabelling could be compared. The approach to standardization could be done using either bench-based techniques or by *in silico* predictions (Guda, 2006; Horton et al., 2007; Nair and Rost, 2005; Nakai and Horton, 1999; Schneider and Fechner, 2004; Shatkay et al., 2007; Hoglund et al., 2006) based on the protein sequences. These approaches have been explored in considerable detail, however, the reliability of the predictions is variable.

In this study we examine the technical aspect of IHC disparity. We propose a workflow for systematic immunolabelling optimization (particularly applicable to previously untested primary antibodies), specifically protocols designed for immunolabelling optimization in formalin-fixed, paraffin wax-embedded (FFPE) material, based on knowledge of the subcellular localization by molecular techniques. In order to achieve this we investigated the use of an independent molecular technique and bioinformatics methods. Specifically, we apply such a methodological approach to five near-novel

Please cite this article as: Mohd Omar MF, et al. Molecular-assisted immunohistochemical optimization. Acta Histochem (2009), doi:10.1016/j.acthis.2009.05.010

antibodies, using a human breast carcinoma cell line, four different antigen retrieval methods and four different concentrations per antibody.

Material and methods

Cell culture and pellet formation

The human breast carcinoma cell line MCF-7 (ATCC: HTB-22) was obtained from the American Type Culture Collection (Rockville, MD, USA), work with this cell line was under NHG Domain-Specific Review Board approval (Reference DSRB-B/09/140). It was cultured in Eagle minimum essential medium, supplemented with 2 mM L-glutamine and Earle's balanced salts solution adjusted to contain 1.5 g/L sodium bicarbonate, 0.1 mM non-essential amino acids, 1 mM sodium pyruvate and 10% fetal bovine serum (Hyclone, Logan, UT, USA). The cells were cultured in a humidified incubator with 5% CO_2 at 37 °C. Cells were grown to confluence, washed in phosphate-buffered saline (PBS) and trypsinized for 5 min to detach cells. The cell suspension was transferred to a 15 mL tube, followed by centrifugation at 1000*g* for 5 min to obtain a cell pellet.

Formalin fixation and paraffin wax embedding (PPFE)

Cells were fixed in 10% neutral-buffered formalin for 30 min at room temperature. Cell pellets were then dehydrated with increasing concentrations of ethanol (70%, 80%, 90% and 100%) for 1 h each and then xylene for a final hour, with centrifugation at 200*g* for 3 min between each step. The cells were then covered in paraffin wax blended with synthetic polymers (congealing temperature 58 °C) (BDH Chemicals Ltd., Poole, Dorset, England) and left overnight at 60 °C. These pellets were then placed into conventional paraffin wax embedding cassettes for sectioning.

Sectioning and immunocytochemistry

The FFPE blocks were sectioned at 4 μm thick and sections mounted on Matsunami adhesive silane (MAS)-coated glass microslides (Superfrost, Matsunami, Tokyo, Japan) and dried overnight at 37 °C. Paraffin wax was removed by three washes in xylene, and the tissue rehydrated in decreasing concentrations of ethanol (100%, 90% and 70%) and water for 5 min each.

The optimization experiments for the five antibodies (Table 1) involved four different antigen retrieval protocols for each antibody. These were performed by immersion of the sections in one of four different buffers (citrate buffer (PC), Tris–EDTA (EDTA), Dako pH 6.0 antigen retrieval buffer (DK6) or Dako pH 9.0 antigen retrieval buffer (DK9) and heating in a pressure cooker (T/T Mega, Milestone) at 120 °C for 5 min. This was followed with incubation with peroxidase block solution (ready-to-use from Dako, Glostrup, Denmark), followed by three rinses in washing buffer (PBS buffer containing 0.1% Tween 20). Five different primary antibodies were used in the study (Table 1), incubated at four different dilutions per antigen retrieval method, namely 1/50, 1/100, 1/200 and 1/400 (diluted with Dako antibody diluent), so that with the variation in antigen retrieval, there were 16 protocols used for each antibody. These five near-novel antibodies (either unused or seldom used for immunohistochemistry previously, and thus with no reliable previous indication of appropriate protocol or immunolabelling distribution) were used in the context of the validation in human clinical samples of a proteomics study in breast cancer cell lines (Ou et al., 2008).

Table 1. Antibody information with chosen protocol for each antibody.

Protein target	Full name	Antibody source	Optimised protocol[a]
6PGL (PGLS)	6-Phosphogluconolactonase	Customized by BioGenes (Berlin, Germany)	EDTA 1/50
CAZ2 (CAPZA2)	F-actin capping protein alpha-2 subunit	Customized by BioGenes (Berlin, Germany)	DK6 1/400
PA2G4 (EBP1)	Proliferated associated protein-2G4	Upstate (Lake Placid, NY, USA)	DK9 1/50
PSD2	26S proteasome non-ATPase regulatory subunit 2	Customized by BioGenes (Berlin, Germany)	DK9 1/200
TKT	Transketolase	Customized by BioGenes (Berlin, Germany)	DK9 1/50

[a]Chosen protocol is the protocol that best reflects the expected results based on the western blots.

Please cite this article as: Mohd Omar MF, et al. Molecular-assisted immunohistochemical optimization. Acta Histochem (2009), doi:10.1016/j.acthis.2009.05.010

Primary antibodies were incubated with sections overnight at room temperature, followed by three rinses in washing buffer. The peroxidase-labelled secondary antibody (EnVision+ kit, Dako, Glostrup, Denmark), prepared according to manufacturer's instructions, was allowed to incubate with the sections for 30 min at room temperature, again followed by three rinses in washing buffer. Antibody binding was detected by a peroxidase-3,3'-diaminobenzidine-based detection system (EnVision+ kit, Dako, Glostrup, Denmark), employed according to kit instructions. The slides were then counterstained with Gill's hematoxylin (Merck Pte. Ltd., Singapore). Finally the slides were dehydrated in increasing concentrations of ethanol (70%, 90% and 100%) for 5 min each, allowed to dry and mounted with a coverslip (Menzel-Gläser, Braunschweig, Germany) using DPX mountant (Fluka, Sigma-Aldrich, Buchs, Switzerland).

Protein extraction and western blot analysis

Protein extraction was performed using the ProteoExtract® Subcellular Proteome Extraction Kit (Calbiochem, EMD Chemicals, Inc., La Jolla, CA, USA), employed according to kit instructions. Briefly, this kit allows the fractionated extraction of the different cellular components, i.e. cytosolic protein, membrane/organelle protein and nucleic protein extracts, based on differing solubilities. Determination of protein concentrations was performed using the Coomassie blue (Bradford) protein assay kit (Pierce, Rockford, IL, USA), according to manufacturer's intructions. SDS-PAGE was performed using a 10% acrylamide gel under standard conditions. A semi-dry transfer was then performed onto a PVDF membrane (Bio-Rad Laboratories (Singapore) Pte. Ltd.) at 15 V for 40 min. The membranes were then blocked with 5% skim milk (Fluka, Sigma-Aldrich, Buchs, Switzerland) in washing buffer. The blots were probed with the antibodies shown in Table 1 at room temperature for 1 h. This was followed by incubation with the secondary antibody (ECL rabbit IgG, horseradish peroxidase-linked whole Ab, GE Pacific Pte Ltd., Singapore) diluted 1/50000 in washing buffer for 1 h. Detection was performed by chemiluminescence using the ECL advance detection kit (GE Pacific Pte Ltd., Singapore), carried out according to kit instructions. The reactivity was visualized on a VersaDoc 5000 (Bio-Rad Laboratories (Singapore) Pte. Ltd.) and analysis of banding using the Quantity One software (Bio-Rad Laboratories (Singapore) Pte. Ltd.).

Scoring of immuncytochemical labelling and comparison to western blot results

Immunolabelling of paraffin wax-embedded sections was scored according to intensity: 0 (negative – no immunolabelling), 1 (mild immunopositivity), 2 (moderate immunopositivity) and 3 (strong immunopositivity), and subcellular localization (nuclear or cytoplasmic). Scoring was performed by a trained scientist (MFMO) and confirmed by a qualified pathologist (MST). To avoid the consideration of non-specific labelling, and to make sure that no false positive results were included in our analysis, only intensities of 2 and 3 were accepted as positive for the purpose of this analysis. Based on the observations, the results were classified into five different categories: (1) even nuclear and cytoplasmic staining, where the intensity of immunolabelling of the nuclear and cytoplasmic components of the cell were both positive and even; (2) primarily nuclear staining, where the nuclear component of the cell was more intensely immunopositive than the cytoplasmic component; (3) primarily cytoplasmic staining, where the cytoplasmic component of the cell was more intensely immunopositive than the nuclear component; (4) variability in nuclear staining, where the immunolabelling in the nucleus varied from cell to cell within the sample; (5) negative for staining, where both the nuclear and cytoplasmic components were unlabelled. Immunopositivity of the western blots are listed as cytoplasmic, membrane/organelle and nucleic, based on the fractionation.

Bioinformatic prediction of protein localization

In order to predict protein localization, three *in silico* animal protein prediction programs were used, specifically Wolf pSORT (Horton et al., 2007), SherLoc (Shatkay et al., 2007) and MultiLoc (Hoglund et al., 2006). Briefly these techniques use prediction algorithms to predict localization of a protein based on structural motifs and signaling sequences. This is achieved by the use of machine learning techniques and the comparison of the protein's sequence against a panel of known proteins from a database (Hoglund et al., 2006; Horton et al., 2007; Shatkay et al., 2007). FASTA format sequences were used for input into the programs. The protein accession numbers for the five protein targets in this study are as follows: O95336 (6PGL), P47755 (CAZA2), Q9UQ80 (PA2G4), Q9BQI7 (PSD2) and P29401 (TKT).

Please cite this article as: Mohd Omar MF, et al. Molecular-assisted immunohistochemical optimization. Acta Histochem (2009), doi:10.1016/j.acthis.2009.05.010

Results

Table 2 summarises the results for all antibody concentrations and antigen retrieval variations of the IHC protocols. Figure 1 illustrates a summary of these results and depicts all the possible immunolabelling variations observed using the five different antibodies. This illustrates the different results that are possible when using a single antibody with different antigen retrieval methods and antibody concentrations. The IHC results indicate a large variability is possible for all the antibodies tested, with immunolabelling ranging from no labelling to either predominantly nuclear or cytoplasmic labelling for any given antibody. It should be noted that not all the antibodies exhibited all immunolabelling

Table 2. Immunolabelling patterns seen using the different protocols.

Antibody target	Dilution of primary antibody	Antigen retrieval using DK6	Antigen retrieval using DK9	Antigen retrieval using EDTA	Antigen retrieval using PC
6PGL	1/50	Primarily cytoplasmic	Primarily cytoplasmic	**Primarily cytoplasmic**	Even nuclear and cytoplasmic
	1/100	Primarily cytoplasmic	Primarily cytoplasmic	Primarily cytoplasmic	Primarily cytoplasmic
	1/200	Primarily cytoplasmic	Primarily cytoplasmic	Primarily cytoplasmic	Variability in nuclear staining
	1/400	Primarily cytoplasmic	Primarily cytoplasmic	Negative for staining	Variability in nuclear staining
CAZ2	1/50	Even nuclear and cytoplasmic	Variability in nuclear staining	Primarily nuclear	Even nuclear and cytoplasmic
	1/100	Even nuclear and cytoplasmic	Variability in nuclear staining	Primarily nuclear	Even nuclear and cytoplasmic
	1/200	Primarily cytoplasmic	Variability in nuclear staining	Variability in nuclear staining	Primarily nuclear
	1/400	**Primarily cytoplasmic**	Negative for staining	Primarily nuclear	Negative for staining
PA2G4	1/50	Even nuclear and cytoplasmic	**Even nuclear and cytoplasmic**	Variability in nuclear staining	Primarily nuclear
	1/100	Variability in nuclear staining	Even nuclear and cytoplasmic	Variability in nuclear staining	Primarily nuclear
	1/200	Primarily cytoplasmic	Even nuclear and cytoplasmic	Variability in nuclear staining	Even nuclear and cytoplasmic
	1/400	Primarily cytoplasmic	Even nuclear and cytoplasmic	Primarily cytoplasmic	Even nuclear and cytoplasmic
PSD2	1/50	Variability in nuclear staining	Even nuclear and cytoplasmic	Primarily cytoplasmic	Primarily nuclear
	1/100	Variability in nuclear staining	Even nuclear and cytoplasmic	Variability in nuclear staining	Primarily nuclear
	1/200	Primarily nuclear	**Even nuclear and cytoplasmic**	Variability in nuclear staining	Primarily nuclear
	1/400	Primarily nuclear	Primarily nuclear	Variability in nuclear staining	Primarily nuclear
TKT	1/50	Primarily nuclear	**Even nuclear and cytoplasmic**	Primarily nuclear	Primarily nuclear
	1/100	Even nuclear and cytoplasmic	Primarily nuclear	Primarily nuclear	Primarily nuclear
	1/200	Even nuclear and cytoplasmic	Primarily nuclear	Primarily nuclear	Primarily nuclear
	1/400	Negative for staining	Primarily nuclear	Primarily nuclear	Negative for staining

The optimal protocol for each antibody, based on its correspondence with the western blot results, are highlighted in bold.

Please cite this article as: Mohd Omar MF, et al. Molecular-assisted immunohistochemical optimization. Acta Histochem (2009), doi:10.1016/j.acthis.2009.05.010

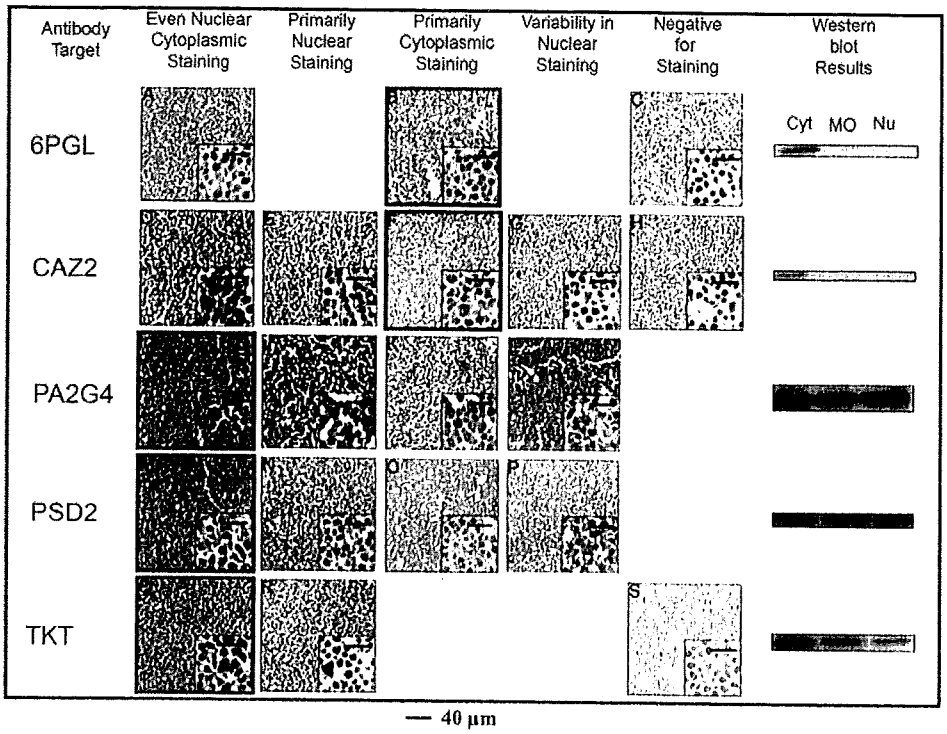

Figure 1. Variation in antibody immunolabelling intensity and localization. Horizontal rows correspond to the antibodies against the different proteins, while vertical columns show the different localization patterns. The results that match the western blot observation are shown with a blue border. The results were categorized into five different possible observations. As shown, the possible outcomes were dependant on the antibody used, i.e. only certain immunolabelling categories were observed for each of the antibodies. The larger image was taken at 100× magnification, whole the panel image was taken at 400× magnification. The protocols used in each case are shown below (antigen retrieval methods followed by the antibody dilution factor) (A) PC, 1/50, (B) EDTA 1/50, (C) EDTA 1/400, (D) PC 1/50, (E) EDTA 1/50, (F) DK6 1/400, (G) DK9 1/50, (H) DK9 1/400, (I) DK9 1/50, (J) PC 1/100, (K) DK6 1/400, (L) EDTA 1/50, (M) DK9 1/200, (N) PC 1/400, (O) EDTA 1/50, (P) EDTA 1/200, (Q) DK9 1/50, (R) DK9 1/400, (S) PC 1/400; PC-citrate buffer, EDTA-Tris-EDTA, DK6-DAKP pH6.0, DK9-DAKO pH 9.0, Cyt – cytosolic fraction, MO – membrane/organelle fraction, Nu – nucleic protein extract.

patterns, for example, CAZ2 exhibits all the immunolabelling variations, while 6PGL and TKT labelled in only three different patterns.

The different antibodies also exhibited varying protein localization patterns and immunolabelling intensities on western blots (Figure 1). 6PGL and CAZ2 labelled only cytoplasmic components, while PA2G4, PSD2 and TKT showed strong labelling in all cellular fractions. The most biologically appropriate immunolocalisation using IHC was judged to be that which corresponded to the western blot result. The IHC results that most closely corresponded to the western blot observations are framed in blue in Figure 1 and highlighted in Table 2. The optimized final protocol for each antibody was different; hence there was no single protocol that was appropriate for all antibodies in the study.

A direct comparison of the three bioinformatics methods used is rather difficult, owing to the different prediction output formats. Table 3 summarises these results, with a standardization of terms when necessary. An overall analysis does, however, reveal that there is no robust agreement between the subcellular localization predictions of the three bioinformatics programs, nor was there an unequivocal correlation of any of the programs with the western blot results.

Discussion

Cell lines serve as the ideal source material for antibody optimization as the derived pellet is a biologically homogenous sample, minimizing the intrinsic variability of the optimization exercise. Cells are relatively easy to manipulate and are a renewable source for multiple optimization and experimentation. For the experimental design, we chose a representative cell line, MCF-7, obtained

Please cite this article as: Mohd Omar MF, et al. Molecular-assisted immunohistochemical optimization. Acta Histochem (2009), doi:10.1016/j.acthis.2009.05.010

Table 3. Comparison of western blot results to WoLF pSORT, SherLoc and MultiLoc2 protein localization predictions.

Antibody	Western blot localization	WoLF pSORT	SherLoc	MultiLoc2
6PGL (PGLS)	Primarily cytoplasmic	Extr: 14.0 Cyto and Nu: 7.7 Nu: 5.5 Mito: 5.0 Cyto and Pero: 4.7 Cyto: 4.5	Cyto: 0.36	Mito: 0.59 Cyto: 0.25 Nu: 0.11 Extr: 0.05
CAZ2 (CAPZA2)	Primarily cytoplasmic	Cyto: 20.5 Cyto and Nu: 14.5 Nu: 5.5 Cysk: 5.0	Cyto: 0.72	Cyto: 0.83 Nu: 0.16 Mito: 0.0 Extr: 0.0
PA2G4 (EBP1)	Even nuclear and cytoplasmic	Nu: 21.5 Cyto and Nu: 15.0 Cyto: 7.5	Nu: 0.93	Cyto: 0.53 Nu: 0.47 Mito: 0.0 Extr: 0.0
PSD2	Even nuclear and cytoplasmic	Plas: 23.0 Er: 6.0	Nu: 0.49	Cyto: 0.78 Nu: 0.21 Mito: 0.01 Extr: 0.0
TKT	Even nuclear and cytoplasmic	Cyto: 18.0 Cytoand Nu: 15.3 Cytoand Plas: 10.2 Nu: 7.5 Er: 3.0	Cyto: 1.0	Cyto: 0.73 Nu: 0.24 Mito: 0.02 Extr: 0.0

Results are shown as rank values that indicate favorability to a specific localization. Higher values indicate a higher likelihood of occurrence at the specific localization site. WoLF pSort and MultLoc2 provide several probable locations for a protein, while SherLoc displays only the most likely localization site. Nu – nuclear, Pero – peroxisomal, Cyto – cytoplasmic, Er – endoplasmic reticulum, Cysk – cytoskeleton, Extr – extracellular, Mito – mitochondrial, Plas-plasma membrane.

from the pleural effusion of a patient with metastatic breast carcinoma (Soule et al., 1973). It is a well characterized estrogen receptor (ER) positive cell line, which is a standard model for the study of breast cancer in laboratories around the world (Lau et al., 2006; Levenson and Jordan, 1997). The cells were formalin-fixed and paraffin wax-embedded to emulate the conditions faced during routine processing and embedding of clinical samples available in conventional pathology departments worldwide. It should be noted that the protein extraction and subsequent western blots were intentionally performed on fresh cells, so as not to introduce any factors that may cause degradation to the protein (Boenisch, 2006). Subsequently, the various optimization protocols were performed using the FFPE material. This approach allowed us to select the protocol for use with FFPE tissue that most closely represented the native state of the protein localization as indicated by the western blots.

As seen in Figure 1 and Table 2, the variation in the immunolabelling patterns of each antibody is very apparent, indicating that the results of any one protocol may be contradictory to the actual protein localization and concentration, and that this is dependent on the antigen retrieval method and primary antibody concentration. The interpretation of this substantial variability for any given antibody ranges from assuming that a protein is not present in a tumor to accepting a functional overexpression of the same protein. This would be very misleading to a researcher and the implication of the incorrect localization patterns would be quite severe in a clinical setting, where inconsistencies could result in incorrect diagnosis, prognosis and treatment.

The introduction of protein from fresh cells and the fractionated western blot analysis was essential in elucidating the biologically correct immunolocalisation pattern, including the subcellular localization which, in itself, dictates the precise functionality of the protein, with the understanding that for practical purposes, cytoplasmic and membranous immunopositivity in the western blot corresponds to general cytoplasmic immunopositivity in IHC.

It should be noted that for each primary antibody, more than one IHC protocol resulted in the

Please cite this article as: Mohd Omar MF, et al. Molecular-assisted immunohistochemical optimization. Acta Histochem (2009), doi:10.1016/j.acthis.2009.05.010

immunolocalisation of the protein consistent with western blot results (Table 1). The number of consistent localizations varied from two different protocols for CAZ2 (primarily cytoplasmic) to as many as 12 different protocols for 6PGL (primarily cytoplasmic). The choice of the most appropriate protocol, consistent with the western blot results, was made by also taking into account the intensity of the IHC labeling; that is, where the immunolabelling intensity values were high, between 2 and 3. An interesting observation is that changes in antigen retrieval buffer appeared to play more of a crucial role in apparent protein subcellular localization rather than primary antibody concentration, and therefore should be of primary concern in an optimization protocol. Without the use of the western blot in an optimization protocol a scientist may have regarded the antibody as optimized with any one of the protocols used, potentially resulting in a drastic difference from actual biological localization of a studied protein. This can be illustrated by the known phenomenon of protein mis-localization and its relevance in protein function. For example, we have shown that subcellular localization of RUNX3 is tightly related to the development of breast cancer (Ito et al., 2005). Others have established its importance in BRCA1 and breast cancer (Rodriguez et al., 2004), in acute promyelocytic leukemia cells that express chimeric RARα fusion proteins (Dong et al., 2004), in human thyroid cancer and p27 (kip1) expression by phosphorylation-dependent cytoplasmic sequestration (Motti et al., 2005) and SRC-1 androgen receptor-dependent nuclear sequestration in prostate cancer (Nazareth et al., 1999), among others.

It is well known that cell lines are prone to genotypic and phenotypic drift during culture, causing the appearance of heterogeneous subpopulations (Burdall et al., 2003; Maitra et al., 2005). Indeed, previous studies have shown that the MCF-7 cell line has shown a high level of clonal variation, including both phenotypic and karyotypic variation (Bahia et al., 2002; Burow et al., 1998; Nugoli et al., 2003; Osborne et al., 1987). This indicates the importance of linking the appearance in western blots and IHC with the knowledge of protein function using a similar passage number and/or origin.

As part of our antibody optimization experiments, we only included the more common and easily altered variables – antigen retrieval method and primary antibody concentration. However, there may be occasions in which adequate results are not obtained by altering these variables alone and then other methodological aspects should be considered, such as, the length of antigen retrieval, the use of different antibody clones detecting different epitopes in the same protein or the molecular optimization using a different cell line. To maintain relative simplicity in the optimization process, we recommend these steps only if necessary, i.e. these factors represent a second line set of variables in the optimization process.

A potential barrier to the use of the approach described here in clinical pathology laboratories is the lack of available cell culture facilities in these routine settings. However, we believe that the cell pelleting protocol described in this paper is simple enough to be carried out in any cytopathology facility and, hence, all that is required from clinical laboratories is to contact research laboratories to acquire the prepared cells with the stipulated characteristics.

In any case, we believe that the lack of access to cell lines and molecular techniques in general by immunohistochemistry-based laboratories may be mitigated, at least in part, in the future. This is so because of the need to combine morphology-based diagnostics with molecular diagnostics in a single laboratory operation. This model on combined morpho-molecular diagnostics will not only be of advantage to the patient and to the pathologist (Salto-Tellez, 2007), but will also make combined approaches for optimization such as the one we are proposing here much more readily available.

As indicated in the small comparative analysis described here, the variation between several well-regarded bioinfomatic predictors of subcellular localization indicate that more work is still necessary before these are readily applied to IHC validation, particularly in the context of clinical immunohistochemistry.

In summary, we have shown that a systematic protocol for IHC optimization, taking into account a parallel mode of protein detection and the functional knowledge of the individual proteins, may improve the consistency of results between different laboratories studying the same proteins and using different antibodies and protocols (McShane et al., 2000; Mengel et al., 2002; Parker et al., 2002; von Wasielewski et al., 2002). Overall, this may also contribute to improving the knowledge of novel proteins in clinical samples and human diseases. With the existing methodology, our study suggests that, to date, the 'standard' used for optimization should preferably be derived by bench-based experiments, rather than bioinformatic prediction techniques.

References

Ainsworth R, Bartlett JM, Going JJ, Mallon EA, Forsyth A, Richmond J, et al. IHC for Her2 with CBE356 antibody

Please cite this article as: Mohd Omar MF, et al. Molecular-assisted immunohistochemical optimization. Acta Histochem (2009), doi:10.1016/j.acthis.2009.05.010